Novel Echocardiographic Techniques in the Diagnosis of Heart Failure

PhD Thesis

By Réka Faludi MD

Head of the Doctoral School: Prof. Sámuel Komoly MD, DSc

Head of the Doctoral Program: Prof. Erzsébet Rőth MD, DSc

Supervisor: Prof. Tamás Simor MD, PhD

Heart Institute

University of Pécs, Pécs, Hungary

2010

Table of Contents

Abbreviations

TDI: tissue Doppler imaging

2D: 2-dimensional

PIV: particle image velocimetry

BNP: B-type natriuretic peptide

PAH: pulmonary arterial hypertension

CTD: connective tissue diseases

PAP: pulmonary artery pressure

HCM: hypertrophic cardiomyopathy

E': early diastolic myocardial longitudinal velocity

A': late diastolic myocardial longitudinal velocity

S: systolic myocardial longitudinal velocity

E: early diastolic velocity of the mitral inflow

A: late diastolic velocity of the mitral inflow

DT: deceleration time of the E wave

IVRT: isovolumic relaxation time

RVFAC: right ventricular fractional area change

PCWP: pulmonary capillary wedge pressure

PVR: pulmonary vascular resistance

ANOVA: analysis of variance

BSA: body surface area

EF: ejection fraction

RV: right ventricle

RS: relative strength

VRS : vortex relative strength

VPC: vortex pulsation correlation

EDWT: end-diastolic wall thickness

LV: left ventricular

EDV: end-diastolic volume

LA: left atrial

MV: mitral valve

ω: vorticity

1. Introduction

1.1. Development of special echocardiographic techniques

Heart failure is a complex clinical syndrome that can result from any structural or functional cardiac disorder that impairs the ability of the ventricle to fill with or eject blood. The syndrome of heart failure is a common manifestation of the later stages of various cardiovascular diseases, including coronary artery disease, systemic or pulmonary hypertension, valvular disease and primary myocardial disease. Echocardiography, what is the most frequently performed cardiovascular examination after electrocardiography, has revolutionized the diagnosis of heart failure. By the help of the common echocardiographic techniques – M-mode, 2-dimensional echocardiography and conventional Doppler – essential information regarding cardiac morphology, function and hemodynamics can be obtained non-invasively. Several challenging problems, however, required the further development of the echocardiographic technique.

The overall function of the left ventricle depends on a normal contraction of the longitudinally and circumferentially orientated myocardial fibers.[1] Quantitation of the left ventricular function in the longitudinal axis may be clinically relevant since the contraction in this direction is mainly due to subendocardial fibers. As the apex of the heart remains remarkably stationary, long axis changes are reflected in movements of the base of the heart. The first detailed data on the analysis of the myocardial dynamics of the heart with the use of pulsed tissue Doppler imaging (TDI) by locating the sample volume at the basal segment of the posterior wall were reported in 1989.[2] By now, TDI has become a validated technique for assessing both regional and global systolic and diastolic myocardial longitudinal function.

Major limitation of the TDI technique is, that cannot differentiate between active and passive movement of a myocardial segment. Myocardial deformation analysis (strain and strain rate) is more useful for detection of regional myocardial dysfunction. Because of the relationship between myocardial motion and deformation, wall motion velocity measurements by tissue Doppler can be used to obtain regional and global strain and strain rate data.[3] Non-Doppler based (2-dimensional- 2D) strain and strain rate imaging is an even newer echocardiographic technique for obtaining deformation measurements.[4] It analyzes motion by tracking speckles (natural acoustic markers) in the 2D ultrasonic image. The geometric shift of each speckle

represents local tissue movement. When frame rate is known, the change in speckle position allows determination of its velocity. Thus, the motion pattern of myocardial tissue is reflected by the motion pattern of speckles. By tracking these speckles, strain and strain rate can be calculated.[4]While traditional and tissue Doppler echocardiography measure velocities relative to the transducer and therefore contain only 1-dimensional information on the blood velocity component towards or away from the transducer, the 2D strain method tracks not along the ultrasound beam, but in two dimensions, along the dimensions of the wall, and thus is angle independent.

Combination of the echocardiographic speckle tracking method and the well-known optical imaging technique of particle image velocimetry (PIV) has made possible the development of a new technique for the visualization of the left ventricular flow pattern. This contrast echocardiography based method is angle independent and therefore is able to provide adequate information for the reconstruction of velocity vector field in the left ventricle.[5-8]

1.2. Special problems in heart failure

Cardiac biomarkers are substances that are released into the blood when the heart is damaged. Measurement of these biomarkers may also help in the diagnosis, evaluation, and monitoring patients with suspected heart failure. B-type (earlier known as “brain”) natriuretic peptide (BNP) has diuretic, natriuretic and vasodilator effects regulating the fluid homeostasis of the human body. The peptide is predominantly secreted by the ventricles of the heart in response to excessive stretching of the cardiomyocytes. BNP is co-secreted along with a 76 amino acid N-terminal fragment (NT-proBNP) which is biologically inactive, but its biological half-life is longer as that of BNP, making this peptide better target than the BNP itself for diagnostic blood testing.[9] The plasma concentration of NT-proBNP is typically increased in patients with asymptomatic or symptomatic left ventricular systolic dysfunction.[10] In patients with isolated left ventricular diastolic dysfunction the NT-proBNP concentration is also elevated, the structural and hemodynamic factors underlying the increase, however, are less clear.[11-13]

Pulmonary arterial hypertension (PAH) is a rare, but life threatening complication of connective tissue diseases (CTD). [14-16] Early detection of CTD patients at risk for pulmonary hypertension could lead to more timely intervention and thus favourably alter disease management. Recent studies suggest that an abnormal rise in pulmonary arterial (PA) systolic pressure (PASP) during exercise in CTD patients is a marker for the development of future

resting PAH.[17-19] Several attempts have been made to find an easy method for recognising patients with stress induced PAH.

The flow inside of the left ventricle represents one of the most interesting but poorly known problems in biological fluid dynamics. A challenging aspect of this topic is the occurrence of diastolic vortices within the ventricular chamber. [20] Such phenomenon has been initially recognised by in vitro experiments, [21] [22]and afterwards confirmed by numerical analysis of the problem.[23-25] In vivo clues in the understanding of the flow features has been obtained by colour Doppler echocardiography [26-28] and by magnetic resonance imaging [29-30] [31-32]both in healthy subjects and under pathologic conditions. Nevertheless, a widespread available method to visualize and quantify left ventricular vortices has not been available so far.

The aim of our work was to prove the usefulness of the novel echocardiographic techniques – TDI and echocardiographic PIV - in the solution of these special problems in heart failure patients.

2. Objectives

- The aim of the study was to investigate the correlation between levels of B-type natriuretic peptide and the TDI and conventional Doppler echocardiographic parameters characterizing the global left ventricular diastolic function in patients with hypertrophic cardiomyopathy.

- Based on non-invasive studies, it has been reported that isolated resting longitudinal diastolic dysfunction of the right ventricle may be the sign of exercise induced pulmonary hypertension in patients with connective tissue diseases. The aim of our work was to confirm this observation by the help of our results obtained from TDI measurements and right heart catheterisation.

- We were planning to describe and distinguish left ventricular flow patterns in healthy hearts and in patients with different types of prosthetic mitral valves by the help of the new method of echocardiographic particle image velocimetry. Flow-mediated energy dissipation in the left ventricle was also investigated.

3. Relationship between conventional and tissue Doppler echocardiographic parameters and B-type natriuretic peptide (NT-proBNP) levels in patients with hypertrophic cardiomyopathy

3.1. Introduction

Hypertrophic cardiomyopathy (HCM) is a hereditary cardiac disease characterized by primary myocardial hypertrophy. The left ventricular cavity is narrow, ejection fraction is normal or supernormal. Left ventricular outflow tract obstruction caused by the hypertrophied interventricular septum occurs in 25% of all HCM patients. Typical symptoms of hypertrophic cardiomyopathy (dyspnoea, decreased exercise capacity) are strongly related to the degree of left ventricular diastolic dysfunction.[33] While several techniques are available to assess left ventricular systolic function, the conventional methods to estimate the left ventricular diastolic function have limited value, because of their dependence on loading conditions.[34-35]

At the same time, TDI has been reported to be a preload independent echocardiographic technique. Early diastolic myocardial velocity (E') measured at the mitral annulus using TDI is a reliable index for evaluating left ventricular diastolic function, while longitudinal systolic velocity (S) is characteristic of global left ventricular systolic function. Late diastolic myocardial velocity (A') is a parameter for assessing left atrial systolic function.[36-38] The ratio of the early diastolic velocity of the mitral inflow to early diastolic velocity of the mitral annulus (E/E') provides a good estimate of left ventricular filling pressure.[33-35, 39]

The plasma concentration of BNP and NT-proBNP is typically increased in patients with isolated left ventricular diastolic dysfunction, the structural and hemodynamic factors underlying the increase, however, are not completely clear.[11-13] Patients suffering from HCM provide a good model to investigate the factors influencing the secretion of this biomarker in isolated left ventricular diastolic dysfunction. Thus the aim of our study was to determine the relation of diastolic mitral annular velocities combined with conventional Doppler indices to the NT-proBNP levels in patients with HCM.

3.2. Patients and methods

3.2.1. Patient selection

Thirty two consecutive patients suffering from HCM were studied. Table 1 outlines the principal characteristics of our patients. The diagnosis of HCM was based on the echocardiographic demonstration of unexplained left ventricular hypertrophy (maximal wall thickness ≥ 15 mm). Patients were selected according to the following criteria: normal sinus rhythm; heart rate < 90 beats/min at the time of the echocardiographic study; absence of mitral stenosis, severe mitral insufficiency or prosthetic mitral valve. Left ventricular ejection fraction was ≥ 50 %, with normal left ventricular cavity dimensions. Usual oral medication of the patients was not discontinued during our studies.

All subjects had given written informed consent prior to undergoing echocardiography and blood sample collection.

Table 1. Main clinical characteristics of the study population

Gender (male/ female)	Age (years)	NYHA functional class	Localization	Outflow tract obstruction (> 30 mmHg)	Medication
21/11	47±14	I. 3 pts. II. 29 pts.	Septal 23 pts Apical 3 pts Cc. 6 pts.	1 pts.	Beta bl. 23pts. ACE-inh. 12 pts. Verapamil 5 pts.

(Pts: patients; cc: concentric; beta bl.: beta blockers; ACE-inh.: ACE-inhibitors)

3.2.2. Echocardiography

All echocardiographic studies were performed using ATL HDI 5000 ultrasound equipment (Bothell, USA) by a single echocardiographer. All 2D and M-mode measurements were obtained from standard parasternal long- and short axis, as well as apical 4- and 2-chamber views. Left ventricular ejection fraction was measured by Simpson's method. Transmitral flow was recorded from the apical 4-chamber view, while placing the sample volume at the level of the mitral valve leaflet tips. Peak of the early (E) and late (A) diastolic velocities and E-wave deceleration time (DT) parameters were measured, and the E/A ratio was calculated.

Isovolumic relaxation time (IVRT) was determined using pulsed Doppler echocardiography. The cursor was placed between the left ventricular outflow and the mitral inflow. TDI of the lateral and septal mitral annulus was also performed in addition to the conventional echocardiographic measurements. Peak of the early- (E') and late (A') diastolic velocities were measured. E/E' ratio was calculated. Measurements were obtained from ≥ 3 consecutive beats. Lateral E/E' >10 or septal E/E' >15 were considered as elevated.[39-40]

3.2.3. Measurement of NT-proBNP

Patients were at rest in supine position for at least 30 min before blood sampling. Peripheral venous blood samples were taken from the antecubital vein at the time of the echocardiography. NT-proBNP levels were detected by immunoassay on the Elecsys 2010 system (Roche Diagnostics). NT-proBNP values increase with age and are higher in women than in men. The following values were considered as normal: in young women (<50 years) <153, in older women < 334, in young men (< 50 years) < 88 and in older men < 227 pg/ml. Precision and analytical sensitivity of the system have already been reported.[41]

3.2.4. Statistical analysis

Continuous variables are presented as mean ± SD. NT-proBNP values did not show normal distribution, thus Spearman's method was used to determine correlations between the continuous variables. Thereafter, the NT-proBNP values were transformed into a natural logarithm (lnNT-proBNP). Stepwise multiple linear regression analysis was performed where lnNT-proBNP served as dependent variable. A p value of < 0.05 was considered significant. Data were analyzed using SPSS 10.0 statistical software (SPSS, Chicago, Illinois).

3.3. Results

Table 2 shows the results of the echocardiographic measurements in our patients. Lateral and septal E/E' indicated elevated left ventricular filling pressure in 10 (31%) and 8 (25%) patients, respectively.

Table 2. Main echocardiographic characteristics of the study population

Parameters	Values measured in HCM-pts
E (cm/s)	76.6±19.8
A (cm/s)	68.9±22.2
E/A	1.2±0.4
DT (ms)	214.7±62.2
IVRT (ms)	101.0±24.5
Lat E' (cm/s)	9.4±3.0
Lat A' (cm/s)	9.0±2.9
E/lat E'	9.1±4.3
Sep E' (cm/s)	6.6±1.8
Sep A' (cm/s)	8.0±2.1
E/sep E'	12.5±4.8

Mean NT-proBNP level turned out to be 543±845 pg/ml. Elevated BNP level was found in 21 patients (66%).

NT-proBNP levels negatively correlated with the lateral ($r=-0.59$, $p<0.001$) and septal ($r=-0.391$, $p=0.03$) A' values and showed a strong correlation with E/A as well ($r=0.476$, $p=0.007$). Weak, but significant correlation was found between the NT-proBNP levels and E/sepE' ($r=0.392$, $p=0.029$). No significant relationship was observed between NT-proBNP levels and other echocardiographic parameters.

By stepwise multiple linear regression analysis the only significant predictor of lnNT-proBNP was lateral A' value, too ($r=-0.467$, $p<0.05$). *(Figure 1.)*

3.4. Discussion

HCM is a typical disease characterized by isolated diastolic dysfunction of the left ventricle. Conventional Doppler echocardiographic assessment of the mitral inflow is dependent on loading conditions, therefore its value is limited in the estimation of the diastolic function.

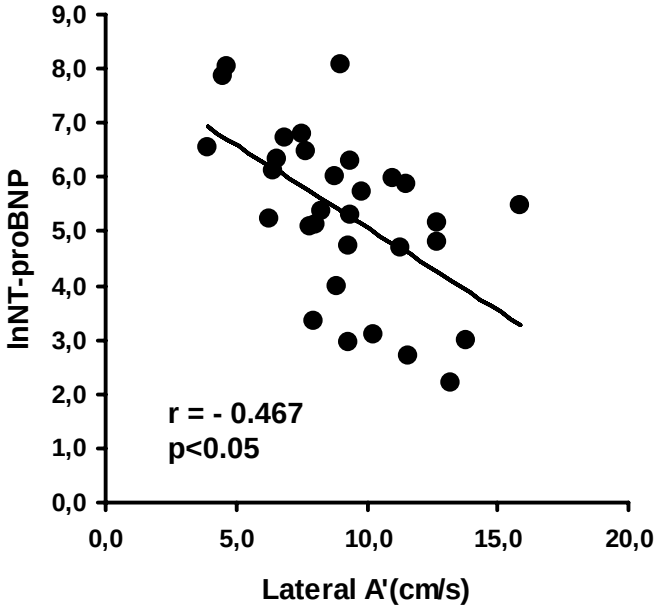

Figure 1. Linear regression between lateral A' and lnNT-proBNP

Doppler curves obtained from the pulmonary veins may serve as a solution for this problem. This measurement, however, is technically challenging, therefore has not become part of the daily routine.[34]

Estimation of the mitral annular motion by the help of TDI is a technically simple and feasible supplementary method for the assessment of the global left ventricular diastolic function. Systolic, early- and late diastolic velocities of the TDI-curve may be obtained from both the lateral and septal region of the mitral annulus. *Nagueh et al.* reported, that in HCM patients lateral E' is higher and more reproducible than septal E', what is often very low in this patient-group.[42] Unfortunately, the normal values of the TDI parameters are not well defined in the literature. Determination of the normal values by age groups seems to be reassuring.[35]

The role of BNP is well known in the diagnosis of the systolic heart failure.[10] Isolated left ventricular diastolic dysfunction is common in conditions such as hypertension, diabetes or chronic ischemic heart disease. Studies to investigate the diagnostic role of the BNP were also performed in these diseases. [11-13] *Mottram et al.* have suggested that the general diagnostic value of BNP is limited in patients with hypertension and consequential left ventricular hypertension. Nevertheless, they have found a significant inverse correlation between BNP

level and the late diastolic TDI parameter (A') measured at the lateral mitral annulus.[12] In HCM patients, *Briguori et al.* could not find any correlation between conventional Doppler-echocardiographic parameters and BNP level. At the same time, they have found significant inverse correlation between the BNP level and left atrial fractional shortening.[11] To date, there are no published data on the relation between BNP level and longitudinal myocardial function in HCM, as determined by TDI.

The aim of our study was to investigate the correlation between NT-proBNP levels and conventional Doppler indices and mitral annular velocities characterizing the left ventricular diastolic function in patients with hypertrophic cardiomyopathy.

According to our results the main determinant of the NT-proBNP level is the A' parameter, characterizing left atrial systolic function. NT-proBNP showed a strong correlation with E/A as well. The latter result, however, must be interpreted carefully, because the E/A ratio does not show a linear correlation with the worsening of the diastolic dysfunction.

The left atrium is a reservoir for the left ventricle during systole, a conduit during early diastole and an active contractile chamber in late diastole. It contributes up to 30% of left ventricular output.[43] During diastole, the left atrium is directly exposed to left ventricular pressure that increases with worsening left ventricular diastolic dysfunction. Consequently, left atrial pressure increases in order to maintain adequate left ventricular filling.[44] This results in increased left atrial wall tension and dilatation of the left atrium. Previous studies have shown a strong association of left atrial volume with left ventricular diastolic function grade.[45-47]

In patients with impaired relaxation (mild form of diastolic dysfunction), the left atrial contractile function and active emptying volume is increased compared with normal, reflecting a compensatory mechanism. As the severity of left ventricular diastolic dysfunction increases (pseudonormal or restrictive filling pattern), this compensatory mechanism is lost, the left atrial contractile function declines parallel with the elevation of left ventricular filling pressure. [12, 44, 48-50]

A' velocity reliably quantifies left atrial contractile function in late diastole.[36-37]. In our study, A' tended to be impaired parallel with the elevation of left ventricular filling pressure, showing a strong inverse correlation with NT-proBNP level.

These data suggests that the missing link between left atrial function and NT-proBNP level may be the left ventricular diastolic function. At the same time, no, or very weak correlations

were found between NT-proBNP and conventional or tissue Doppler parameters characterizing the global left ventricular diastolic function (DT, IVRT, E') or left ventricular filling pressure (E/E').

Previous studies reported that BNP is secreted predominantly from the ventricle and the principal factor stimulating BNP synthesis and release from the ventricular cardiomyocytes is the increased ventricular wall stress.[10] Our data, however, suggests that left atrial wall stress may be an additional, direct determinant of the BNP synthesis. Further studies are necessary to elucidate this phenomenon. In addition, the predictive value of the easily measurable A' parameter should be further evaluated in larger outcome studies.

4. Echocardiographic monitoring of right ventricular function in patients with resting or stress induced pulmonary arterial hypertension secondary to connective tissue diseases

4.1. Introduction

PAH is a rare disease of small pulmonary arteries characterised by endothelial dysfunction and cellular proliferation throughout all vessel layers, resulting in progressively elevated pulmonary arterial resistance with increasing right heart strain and finally right heart failure. The condition may develop in CTD such as systemic sclerosis, systemic lupus erythematosus, mixed connective tissue disease, and to a lesser extent, rheumatoid arthritis, polymyositis and primary Sjögren's syndrome leading to a substantial worsening of prognosis. The survival rate of CTD patients with PAH is in the range of some malignant diseases and highlights the need for early diagnosis and treatment. [14-16]

Early detection of CTD patients at risk for pulmonary hypertension could lead to more timely intervention and thus favourably alter disease management. The change in PASP with exercise provides a possible tool for such detection. In normal individuals, PA pressures remain unchanged with exercise or increase slightly. Although the concept of exercise induced PAH has been eliminated from the recent guideline, [51] several studies suggest that an abnormal rise in PASP during exercise in CTD patients with or without exertional dyspnoea, but with normal resting PA pressures, is a marker for the development of future resting PAH.[17-19]

The most commonly used method to identify CTD patients with exercise induced PAH is the exercise Doppler echocardiography. Nevertheless, a recent study based on resting pulsed-tissue Doppler echocardiography showed that in systemic sclerosis patients a predominantly diastolic right ventricular dysfunction may be found, also in the presence of normal resting PASP, probably as the consequence of the exercise induced PAH.[52] Based on stress echocardiography and resting TDI measurements *Huez et al*.[53] also suggested that isolated resting longitudinal diastolic dysfunction of the right ventricle may be the sign of exercise induced pulmonary hypertension. The aim of our work was to confirm this observation by the help of our data obtained by TDI measurements and right heart catheterisation.

4.2. Methods

4.2.2. Study population

A total of 60 patients (mean age 54±8 years, 50 female) were enrolled into the study. These comprised 15 healthy subjects who had no signs or symptoms of heart disease and 45 consecutive patients suffering from CTD of whom 40 had systemic sclerosis, 2 had systemic lupus erythematosus, 2 had mixed CTD and 1 had polymyositis. Patients in the latter group were referred to our institution on suspicion of PAH, because of complaints of exertional dyspnoea.

Patients with tachycardia (> 90 beats/min), systemic hypertension (blood pressure > 140/90 mmHg), impaired left ventricular systolic function (ejection fraction < 50%), atrial fibrillation, tricuspid stenosis or with significant left sided valvular abnormalities were excluded from the study.

The national ethics committee approved the study. All subjects had given written informed consent prior to undergoing echocardiography and right heart catheterization.

4.2.3. Echocardiography

Echocardiography was performed using Aloka ProSound 5500 ultrasound system (Aloka Co. Ltd, Tokyo, Japan). Left ventricular ejection fraction was measured by Simpson's method. Right ventricular end-diastolic diameter was obtained from standard parasternal long axis view using M-mode measurements. Right ventricular end-systolic and end-diastolic areas were measured in apical 4-chamber view. Right ventricular fractional area change (RVFAC) was calculated as the difference between the two areas, expressed as the percentage of the end-diastolic area. Transmitral and transtricuspid flows were recorded from the apical 4-chamber view. Peak of the early (E) and late (A) diastolic velocities were measured. Systolic pulmonary artery pressure (PAP) was estimated as a sum of the pressure difference across the tricuspid valve calculated using the modified Bernoulli equation and an estimate of mean right atrial pressure (5 to 15 mmHg) using the diameter and collapse index of the inferior vena cava. Myocardial systolic (S), early (E') and late (A') diastolic velocities were measured from apical 4-chamber view at the lateral border of the mitral and tricuspid annulus using pulsed TDI. Tricuspid E/A and mitral E/E' ratios were calculated. Doppler measurements were obtained from ≥ 3 consecutive beats during end-expiratory apnoea.

4.2.4. Right heart catheterization

All patients with CTD underwent right heart catheterization. Echocardiography and catheterization were performed within an interval of five days. A 7Fr Swan-Ganz catheter was introduced to a main pulmonary artery branch. If the resting mean PAP was lower than 30 mmHg, a 3 minutes bench-fly physical stress test was performed using two 1-kg dumbbells. Mean and systolic and diastolic PAP was measured at rest and at peak exercise. Mean PAP >25 mmHg at rest or >30 mmHg at exertion were considered as elevated. PAH was diagnosed if at the same time pulmonary capillary wedge pressure was <15 mmHg at rest.

4.2.5. Statistical analysis

Continuous variables are presented as mean ± SD. Differences between groups were tested for significance using analysis of variance (ANOVA). Post hoc tests were performed by Bonferroni method. Comparisons of non-parametric data were performed by chi^2 tests. A p value of < 0.05 was considered as significant. Data were analyzed using SPSS 13.0 statistical software (SPSS, Chicago, Illinois).

To determine the intraobserver variability, one observer analyzed the TDI variables twice, blinded to the results of the first measurements. Intraobserver variability was expressed as the difference between the measurements/mean of the measurements x 100.

4.3. Results

13 patients belonging to the CTD-group had resting, while 8 patients had only stress induced PAH diagnosed by right heart catheterization (Table 3). Invasively measured mean and systolic PAP both showed a strong correlation with the systolic PAP estimated by echocardiography (mean PAP: $r = 0.685$, $p<0.001$; systolic PAP: $r = 0.615$, $p<0.001$).

Considering the result of the right heart catheterization, CTD patients were divided into the following three groups: 24 patients without PAH, 8 patients with stress induced PAH and 13 patients with resting PAH. Table 4 outlines the principal clinical and echocardiographic characteristics of our patient-groups. The four groups were matched in age, gender distribution and body surface area. The left ventricular ejection fraction was significantly lower in patients with resting PAH than in the other groups, but the difference was clinically insignificant.

Table 3. Hemodynamic data obtained by right heart catheterization in CTD patients

	Patients with CTD (n=45)		
	Without PAH (n=24)	**Stress induced PAH (n=8)**	**Resting PAH (n=13)**
Resting mean PAP (mmHg)	18.0±3.2	22.8±1.7	37.9±10.9
Mean PAP at peak exertion (mmHg)	22.4±4.6	39.8±6.3	
PCWP (mmHg)	11.2±3.2	13.9±0.5	13.1±2.1
PVR (dyn*sec/cm^5)	116.8±68.8	137.6±48	351.2±112.0

(PCWP: pulmonary capillary wedge pressure; PVR: pulmonary vascular resistance)

In healthy subjects preserved left ventricular diastolic function (E/A>1, normal mitral E'), while in CTD patients predominantly impaired relaxation (E/A<1, reduced mitral E') was found. No significant difference was found between mitral E/E' values in the four groups. Diameter of the right ventricle was significantly larger in patients with resting PAH than in subjects in the other three groups.

Based on TDI measurements, in patients with stress induced PAH isolated diastolic right ventricular dysfunction was found, while patients with resting PAH had a combination of systolic and diastolic dysfunction. Tricuspid E/A and RVFAC results confirmed these findings.

TDI measurements were feasible in all patients. In two patients with CTD prior modification of chronotropic therapy was necessary before including to the study by reason of severe tachycardia. Intraobserver variability was 0.43 cm/s (4.5%) for tricuspid E', 0.51 cm/s (3.9%) for tricuspid A' and 0.37 cm/s (2.9%) for tricuspid S.

Table 4. Main clinical and echocardiographic characteristics of the study population

	Normal subjects (n=15)	Patients with CTD (n=45)			p
		Without PAH (n=24)	Stress induced PAH (n=8)	Resting PAH (n=13)	
Age (years)	50±6	54±7	58±8	55±8	NS
BSA (m^2)	1.74±0.15	1.76±0.16	1.76±0.14	1.71±0.26	NS
Male/Female	3/12	3/21	0/8	4/9	NS
NYHA class					
I	15				<0.001
II		24	8	7	
III				6	
Left ventricular EF (%)	63.5±2.3*	61.2±3.3	63.1±2.5#	59.0±3.7	<0.01
Mitral E/A	1.3±0.4	1.0±0.3	0.9±0.3	1.1±0.3	NS
Mitral E' (cm/s)	12.1±2.5	9.9±2.5§	9.2±1.3§	9.4±1.4§	<0.01
Mitral E/E'	5.9±1.3	7.1±2.4	8.0±1.2	7.9±2.6	NS
RV diameter (mm)	27.9±2.5†	31.8±4.1*	28.6±3.7†	38.4±8.2	<0.001
RVFAC (%)	56.9±4.6†	53.7±4.1†	54.8±3.7†	41.4±5.5	<0.001
Tricuspid E/A	1.37±0.21	1.20±0.28	0.91±0.17‡	0.97±0.09‡	<0.001
PASP estimated (mmHg)	24.6±2.4†	30.0±7.0†	32.8±4.5†	52.7±18.7	<0.001
Tricuspid S (cm/s)	13.9±2.6*	13.1±2.7#	12.7±2.1	10.6±2.4	<0.01
Tricuspid E' (cm/s)	11.0±1.7	9.7±2.3	8.2±2.2§	8.4±1.1§	<0.01
Tricuspid A' (cm/s)	13.4±3.0	13.7±2.8	12.8±2.4	12.0±3.6	NS
Tricuspid E'/A'	0.86±0.25	0.72±0.19	0.67±0.24	0.76±0.22	NS

(BSA: body surface area; EF: ejection fraction; RV: right ventricle; RVFAC: right ventricular fractional area change; PASP estimated: systolic pulmonary artery pressure estimated by echocardiography; #p<0.05 versus resting PAH; *p<0.01 versus resting PAH; †p<0.001 versus resting PAH; §p<0.01 versus normal; ‡p<0.001 versus normal)

4.4. Discussion

Exercise capacity in CTD patients without PAH may be decreased due to skeletal muscle involvement, deconditioning or – very often – due to left ventricular diastolic dysfunction.[54] Diastolic dysfunction (predominantly impaired relaxation) was typical in all groups of our CTD patients, the left ventricular filling pressure, however, was not elevated.

Combination of elevated PAP and normal left ventricular filling pressure is characteristic of arterial (pre-capillary) pulmonary hypertension, which is a severe, potentially life-threatening complication of CTD. The pathophysiologic mechanisms leading to PAH and consequentially to right heart dysfunction are thought to be similar in patients with CTD.[14-16]

Determination of the tricuspid annular velocities provides an excellent tool for assessing the global systolic and diastolic function of the right ventricle. [55-56] The long axis function is guided by subendocardial fibres, which are most vulnerable to transitional or permanent pressure overload in patients with stress induced or resting PAH. Our results - based on invasive and TDI measurements - confirmed the observation of *Huez et al* .[53] suggesting that the isolated diastolic dysfunction of the right ventricle is the sign of stress induced pulmonary hypertension. In patients with resting elevation of pulmonary artery pressure combined systolic and diastolic dysfunction was found. *(Figure 2.)* The latter observation is in accordance with the result reported by *Ruan and Nagueh* regarding patients with idiopathic pulmonary hypertension. [57]

Elevated ventricular pressure, however, is not the only possible cause of the right ventricular dysfunction in patients with CTD. Disturbances of myocardial microcirculation and interstitial fibrosis as the hallmarks of primary myocardial involvement may also damage the function of the subendocardial fibres. [58] Nevertheless, TDI seems to be a promising new method to confirm or eliminate suspicion of stress induced pulmonary hypertension in patients with connective tissue disease when the non-invasively estimated pulmonary artery pressure is normal at rest.

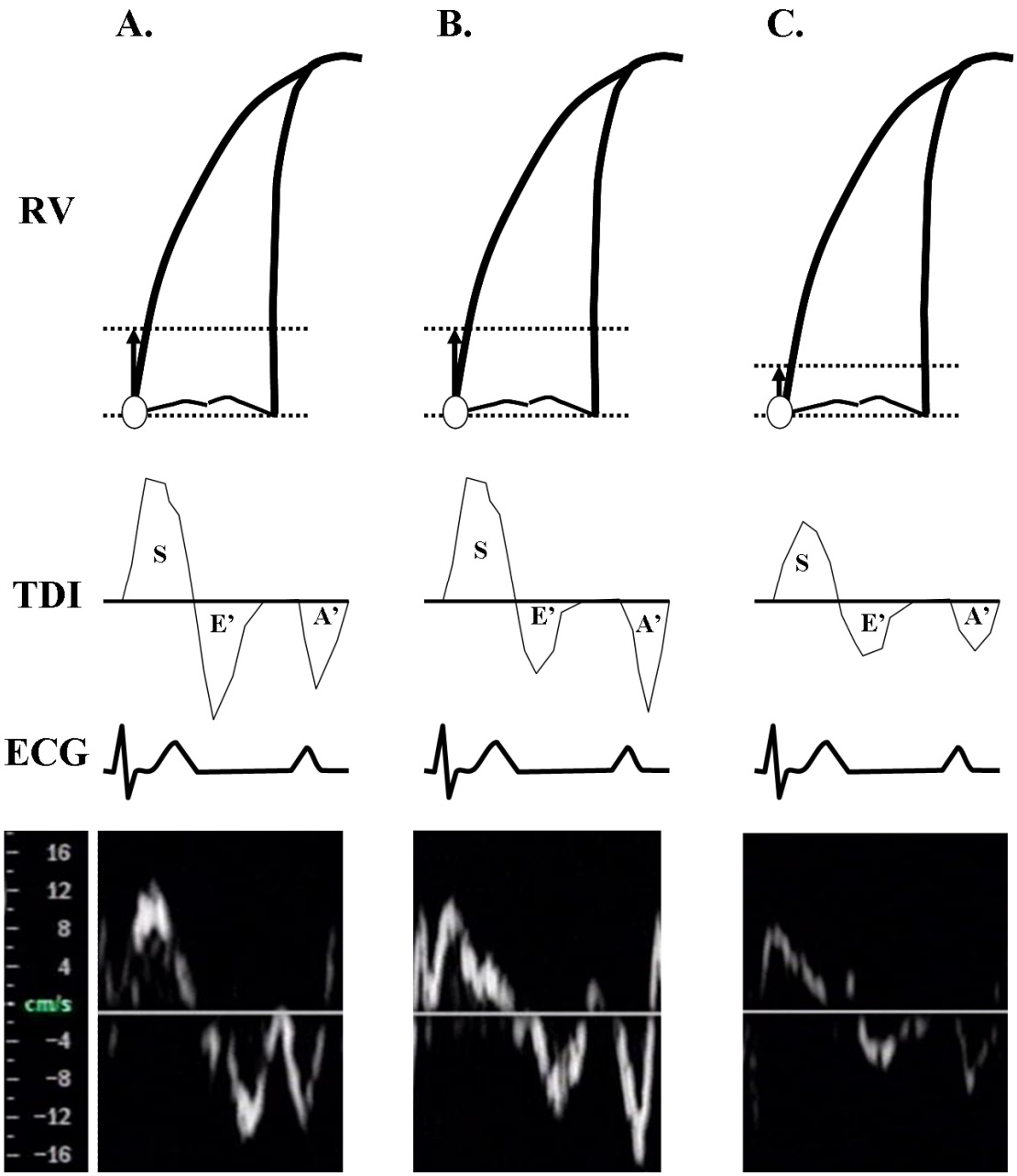

Figure 2. Schematic drawing of the tricuspid annular motion (RV) and the typical tissue Doppler curve obtained at the tricuspid annulus (TDI) in healthy subjects (A), patients with stress induced PAH (B) and in patients with resting PAH (C).

5. Echocardiographic particle image velocimetry: a new method to determine left ventricular flow pattern

5.1. Introduction

5.1.1. Intraventricular flow patterns after mitral valve replacement

The transvalvular flow characteristics of commonly used mitral prosthetic valves are well known. [59] The intraventricular vortex formation in relation to the type and orientation of the mitral valve prosthesis, however, has not received the same clinical attention. Several factors influencing outcomes in mitral valve replacement have been reported. [60-61] Nevertheless, the wide variance in postoperative ejection fraction and in survival rate of patient after mitral valve replacement remained partially unexplained. To what extent changes in intracavitary blood flow patterns contribute could not be measured so far and remains to be determined.

5.1.2. Characterization of flow patterns

Flow can be described as laminar, vortical, or turbulent. Although laminar flow, which can occur in straight blood vessels, is characterized by parallel stream lines, vortical and turbulent flows are dominated by swirling motion of the fluid at different scales. In the 15th century, Leonardo da Vinci pictured vortices in the sinuses above the aortic valve.[62] Until today, vortices in the human circulation remain a challenging aspect of fluid dynamics. Modern phase-contrast magnetic resonance imaging (MRI) has shown that vortical flow is a common finding in the human heart,[20, 29-30, 63-64]as well as in the great arteries.[65-66] Vortices are created when the boundary layer of a fluid detaches from a sharp edge.[67] In the left ventricle laminar mitral inflow is converted into a vortex formation at the tips of the mitral valve leaflets. This vortex formation maintains the momentum of the blood and allows smooth redirection of blood flow toward the outflow tract during systole with minimal generation of turbulence, thus avoiding large losses of kinetic energy.[20, 25, 68]

Vortical flow can be characterized by the quantity vorticity (ω) as follows:

(1) $$\omega = \frac{\Delta v_y}{\Delta v_x} - \frac{\Delta v_x}{\Delta v_y}$$

In a 2-dimensional flow field, vorticity (ω) may be calculated as the difference of the gradient of the y-component of the flow velocity in x-direction $\left(\frac{\Delta v_y}{\Delta v_x}\right)$ and the gradient of the x-component of the flow velocity in y-direction $\left(\frac{\Delta v_x}{\Delta v_y}\right)$.Therefore, vorticity is positive if a vortex rotates counter clockwise; it is negative with clockwise rotation. Laminar flow has a zero vorticity (*Figure 3.*).[67]

Because of fluid viscosity, a vortex looses energy. This energy loss is particularly high if there are rapid changes in vorticity (high pulsatility) or if many small vortices interact (turbulence). In other words, a single, big and steady vortex is an energetically favourable condition, while splitting the bloodstream into smaller, rapidly changing vortices is unfavourable:[67] Kinetic energy gets lost which needs to be provided again by the ventricular musculature.

Changes in regional vorticity can be used to estimate energy dissipation in the fluid. They may be expressed relative to the steady vorticity component in order to obtain a dimensionless parameter. This relative strength of the pulsatile component of vorticity can be calculated for the entire ventricle (RS) or for the vortex region alone (VRS). RS and VRS are here defined as

(2) $$RS = \frac{\int_{LV} \omega_1(x,y)dxdy}{\int_{vortex} \omega_0(x,y)dxdy}$$

(3) $$VRS = \frac{\int_{vortex} \omega_1(x,y)dxdy}{\int_{vortex} \omega_0(x,y)dxdy}$$

where ω_0 represents the steady, and ω_1 the pulsatile component (first harmonic) of regional vorticity.[67]

Conceptually similar, but with a different mathematical definition, the vortex pulsation correlation (VPC) can be calculated as

(4) $$VPC = \frac{A_{vortex} \int_{vortex} \omega_0(x,y)\omega_1(x,y)dxdy}{\left(\int_{vortex} \omega_0(x,y)dxdy\right)^2}$$

where ω_0 represents again the steady, and ω_1 the pulsatile component (first harmonic) of regional vorticity, and A_{vortex} the vortex area.[67]

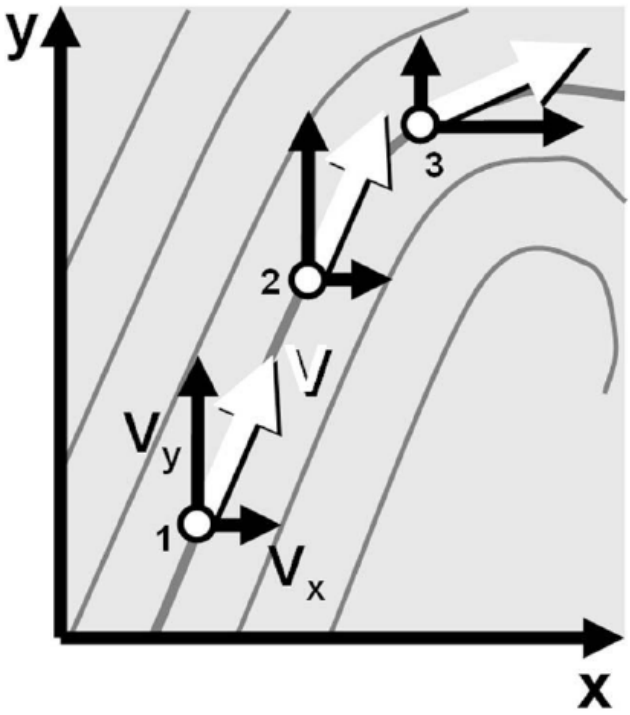

Figure 3. Definition of vorticity in two dimensions. Vorticity is a measure of the curl of streamlines (gray lines) of a fluid. According to equation (1), vorticity will be zero (laminar flow) if calculated between points 1 and 2, and it will be negative if calculated between points 2 and 3 (clockwise rotation). (v: flow velocity; vx,vy: x- and y-components of the flow velocity)

5.1.3. Particle image velocimetry

Traditional spectral- or colour Doppler echocardiography measures velocities relative to the transducer. Doppler data therefore contain only 1-dimensional information on the blood velocity component towards or away from the transducer and do not allow assessment of the direction of blood flow.

Particle image velocimetry (PIV) is a well known principle of determining velocity and direction of fluid streams by analyzing the change in position of small particles that drift with the fluid to be investigated.[69]With the recent development of echocardiographic speckle tracking technology it is now possible to apply this approach to echocardiographic imaging.[6-8]

Blood flow can be tracked after administration of a low dose of contrast. Intracavitary blood flow patterns may then be visualized and quantified in the two dimensions of the image plane.

In this study we use the new echocardiographic PIV method to investigate the influence of mitral valve replacement therapy on blood flow patterns in the left ventricular cavity.

5.2. Materials and methods

5.2.1. Study Population

We examined 19 patients (mean age, 57±19 years; 10 female patients). Nine were healthy volunteers without signs or symptoms of heart disease. Ten patients had prosthetic mitral valves (5 bi-leaflet valves [29-33 mm, St Jude; St Jude Medical, St. Paul, Minnesota] in anatomic orientation, 4 bioprostheses [29–33 mm, Carpentier–Edwards; Edwards Lifesciences, Irvine, California], and 1 tilting-disc valve [Medtronic Hall, 29 mm; Medtronic, Minneapolis, Minnesota] with anterior orientation of the greater orifice). Patients with atrial fibrillation, segmental wall motion abnormalities, or impaired left ventricular systolic function (regional wall motion abnormalities or ejection fraction<50%) were not included. Six patients had medically treated arterial hypertension. The local ethics committee approved the study. All subjects provided written informed consent before inclusion.

5.2.2. Echocardiographic image acquisition

Subjects were imaged in a supine position by using an Acuson Sequoia C512 ultrasound system (Siemens Medical Solutions, Mountain View, California). In addition to a standard echocardiogram, 2-dimensional greyscale images were acquired with high frame rate (80–100/s) in all 3 standard apical views and repeated intravenous administration of a low dose of left heart contrast (0.1–0.2 ml of SonoVue). The mechanical index was set to 0.5 to 0.8 to avoid apical contrast bubble destruction. Images were acquired when cavity contrast distribution was homogeneous and single contrast bubbles could be distinguished. Image loops of 3 cardiac cycles were digitally stored for subsequent offline analysis.

5.2.3. Data Analysis

Conventional 2-dimensional and Doppler recordings were analyzed during the examination or with a dedicated workstation (Syngo, Siemens Medical Solutions, Mountain View, California). We measured left ventricular volumes and ejection fractions using a biplane Simpson's approach, as well as left ventricular and left atrial dimensions and the prosthetic mitral valve gradient.

5.2.4. Particle image velocimetry

Echocardiographic loops were processed offline by using a dedicated prototype software (Omega Flow Version 2.3.1., Siemens). At first, the endocardial border was manually traced in one still frame and then automatically tracked by the software during the cardiac cycle. In a second step the so-defined cavity area was analyzed with a feature tracking algorithm. Contrast bubbles were assumed to move with the blood flow, and thus tracking them allowed us to obtain regional flow information (by means of PIV). Third, the software analyzed the left ventricular cavitary flow field and derived parameters to describe flow patterns. The maximal vortex area during diastole was given in percentages of the left ventricular area. If two vortices were present, the sizes were added. Estimates of energy dissipation (RS, VRS, and VPC) were retrieved. Flow patterns were visually assessed by interpreting a field of flow velocity vectors superimposed on the grey scale image loops. Colour-coded images visualized the flow patterns averaged over the cardiac cycle.

5.2.5. Statistical analysis

Continuous variables are presented as means ± standard deviations. Differences between two groups were tested for significance by using the unpaired *t* test. For more than two groups, analysis of variance (ANOVA) with a Bonferroni post hoc test was used. Contingency tables were analyzed with a chi^2 test. Mean standard deviations between readings were calculated to assess reproducibility of data analysis. Data were analyzed with SPSS 13.0 software (SPSS, Inc, Chicago, Illinois).

5.3. Results

5.3.1. Patient data, feasibility, and reproducibility

Table 5 summarizes the characteristics of our study population. Patients were significantly older than the healthy subjects. No significant differences were found between the groups regarding sex distribution, body surface area, ejection fraction, or left ventricular end-diastolic volume. Left atrial area and mean mitral valve gradient were significantly larger in patients with prosthetic mitral valves.

Table 5 Clinical and echocardiographic characteristics of our study population

	Healthy subjects (n=9)	**Patients with prosthetic MV (n=10)**	***p***
Age (years)	40±11	72±6	**0.000**
BSA (m^2)	1.82±0.29	1.81±0.16	0.972
Male/Female	4/5	5/5	0.808
EDWT septum (mm)	8.9±1.1	11.7±2.2	**0.003**
EDWT lateral wall (mm)	9.3±1.3	11.1±1.3	**0.009**
LV EDV/BSA (ml/m^2)	52.8±9.1	50.9±8.7	0.643
LV EF (%)	61.6±6.8	59.7±7.6	0.079
LA area/BSA (cm^2/m^2)	9.1±1.3	15.0±2.3	**0.000**
Mean MV gradient (mmHg)	0.8±0.3	4.5±2.0	**0.000**

(BSA: body surface area; EDWT: end-diastolic wall thickness; LV: left ventricular; EDV: end-diastolic volume; EF: ejection fraction; LA: left atrial; MV: mitral valve)

Because of severe emphysema, acquisition of a 3-chamber view was not possible in one patient with a prosthetic mitral valve. Otherwise, offline analysis of left ventricular cavitary blood flow patterns was feasible in all subjects. Parameters of vortex area and energy dissipation showed low intraobserver variability: standard deviations between three repeated readings were 3.7%, 6.0%, 5.7%, and 6.2% for RS, VRS, VPC and vortex area, respectively.

5.3.2. Flow patterns in healthy subjects

In all healthy subjects, we found a vortex that detaches from the anterior leaflet of the mitral valve early after the peak of the E-wave *(Figure 4., A)*. This vortex rotates counter clockwise in the 4-chamber view and clockwise in the 3-chamber view and fills almost the entire left ventricle by the end of the E-wave *(Figure 4., B)*. With atrial contraction, late mitral inflow is directed more laterally and generates a second smaller vortex with equal rotation direction in the basal half of the left ventricle *(Figure 4., C)*. With the beginning of systole, the rotating blood is redirected toward the outflow tract *(Figure 4., D)*. Laminar flow is noted when blood leaves the left ventricle. *Figure 4., E* and *G*, shows the spatial vorticity distribution of the left ventricle averaged over the cardiac cycle.

Quantitative parameters of energy dissipation are summarized in Table 6 RS and VPC values were significantly lower in healthy hearts than in patients with prosthetic valves, whereas the maximal vortex size did not differ between the groups.

5.3.3. Flow patterns of bi-leaflet valves in anatomic orientation

5.3.3.1. General pattern

All patients had their bi-leaflet prostheses implanted in anatomic orientation (ie, with the hinge positions approximating commissures of the previous native valve). The two outer orifices generate jets directed toward the left ventricular septum and the lateral wall. In the 4-chamber view the contrast bubbles of the septal jet reach the apex first, whereas those of the lateral jet travel slower *(Figure 5., A)*. Subsequently, during the deceleration of the E-wave, the septal jet becomes dominant *(Figure 5., B)* and forms a major vortex by the end of the diastole, rotating clockwise in the 4-chamber view *(Figure 5., C)*. Thus with the beginning of systole, outflowing blood crosses the previous inflow area *(Figure 5., D)*. In general, the resulting vorticity pattern in hearts of patients with bi-leaflet valves is opposite to that seen in healthy hearts: a large clockwise rotating vortex can be seen in blue in the 4-chamber view *(Figure 5., E)* whereas the 3-chamber view shows a counter clockwise rotating vortex in red *(Figure 5., G)*.

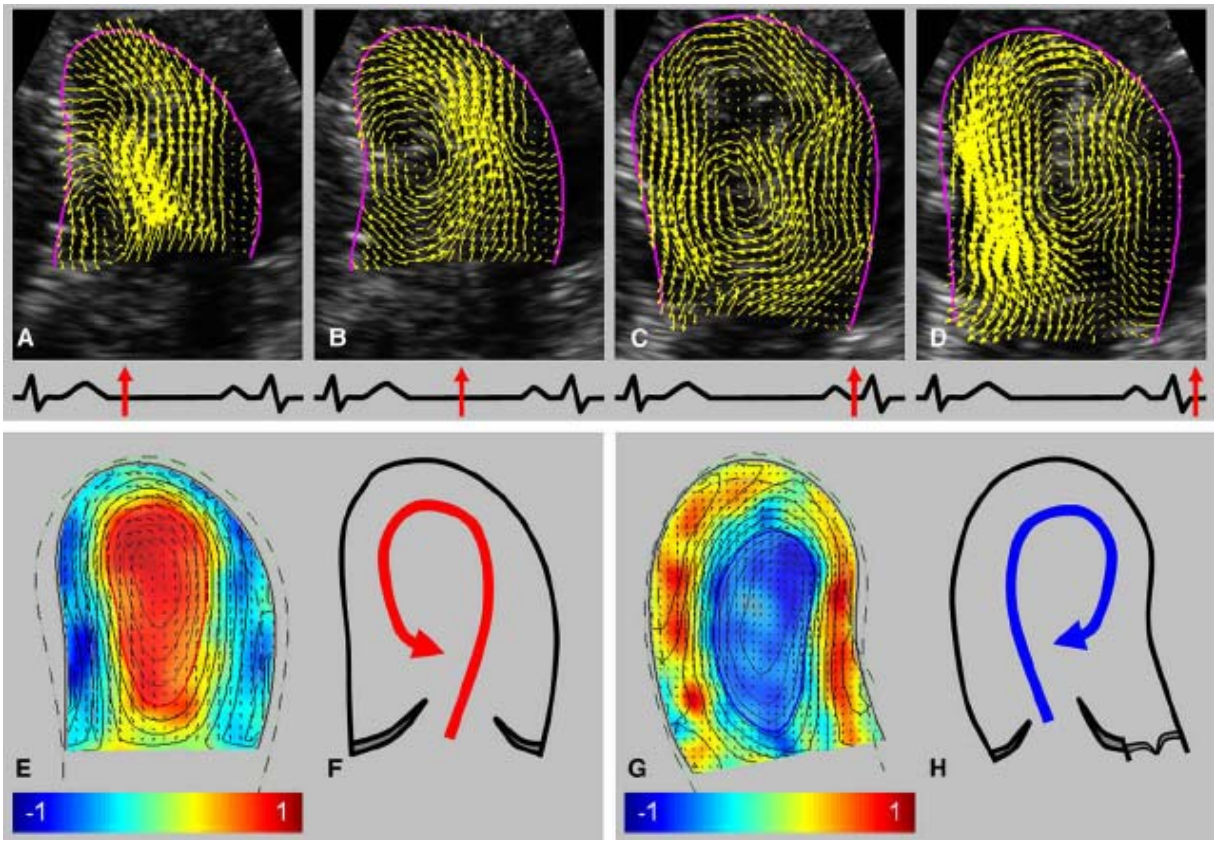

Figure 4. Flow pattern in a healthy left ventricle. Yellow arrows indicating the instantaneous local direction and velocity of blood flow are superimposed on a contrast-enhanced greyscale image of a 4-chamber view. A-D, see text for description of the temporal sequence. ECG was used as a time reference.

Normalized regional vorticity in the plane of the 4-chamber view is averaged over the cardiac cycle. Counter clockwise rotation of the blood (positive vorticity) is colour-coded in red (E), and clockwise rotation is colour-coded (negative vorticity) in blue (G). Schematic drawings of the dominating flow path as observed during diastole are shown (F,H). G and H: same display as E and F but a 3-chamber view. Note that in images E and F, the central vortex is surrounded by a colour rim indicating an opposite vorticity. This is explained by blood velocities, which gradually increase from the endocardium toward the vortex structure. Such a velocity gradient can be interpreted as vorticity and is thus colour-coded.

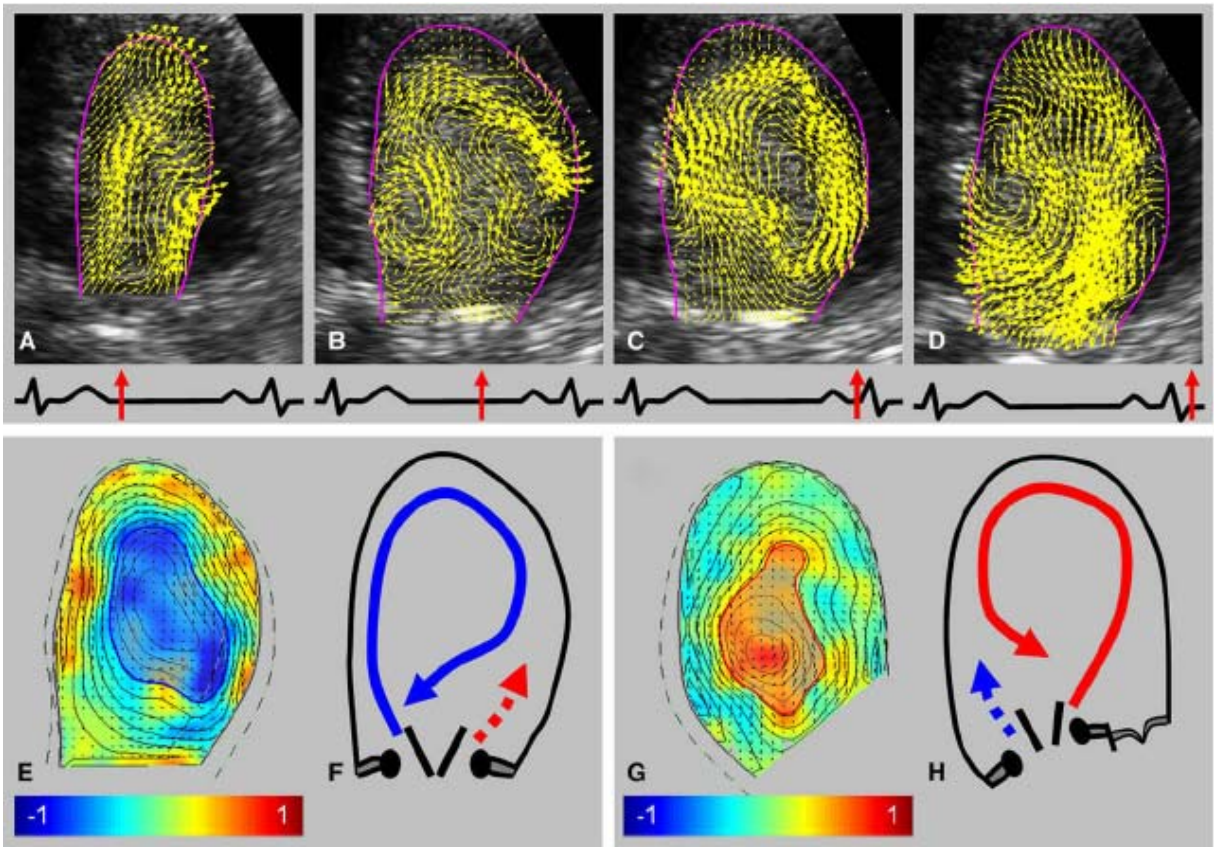

Figure 5. General flow pattern in patients with bi-leaflet mitral valve prosthesis in anatomic orientation. There is a similar display as in Figure 5.2. See the text for a detailed description.

5.3.3.2. Influence of left ventricular geometry

Two patients with bi-leaflet mitral valve prostheses had a marked midseptal hypertrophy (maximal wall thickness, 14 and 15 mm, respectively). In those patients the septal jet did not reach the apex directly but was redirected toward the lateral wall by the hypertrophied septum. From there, it split into two streams forming two counterrotating vortices: a clockwise rotating vortex in the basal half of the ventricle and a second, counter clockwise rotating vortex in the apex *(Figure 6., A and C, upper panels)*. With the beginning of systole, outflowing blood again crosses the previous inflow area *(Figure 6., B, upper panel)*. *Figure 6., D (upper panel)* provides a schematic drawing of the main flow paths.

Parameters of energy dissipation (RS and VPC) were significantly higher in patients with bi-leaflet valves than in healthy subjects (Table 6). Compared with patients with bi-leaflet valves with the general flow pattern, RS tended to be particularly high in those with altered left ventricular geometry (1.98±0.82 vs. 2.85±0.90, p=0.171).

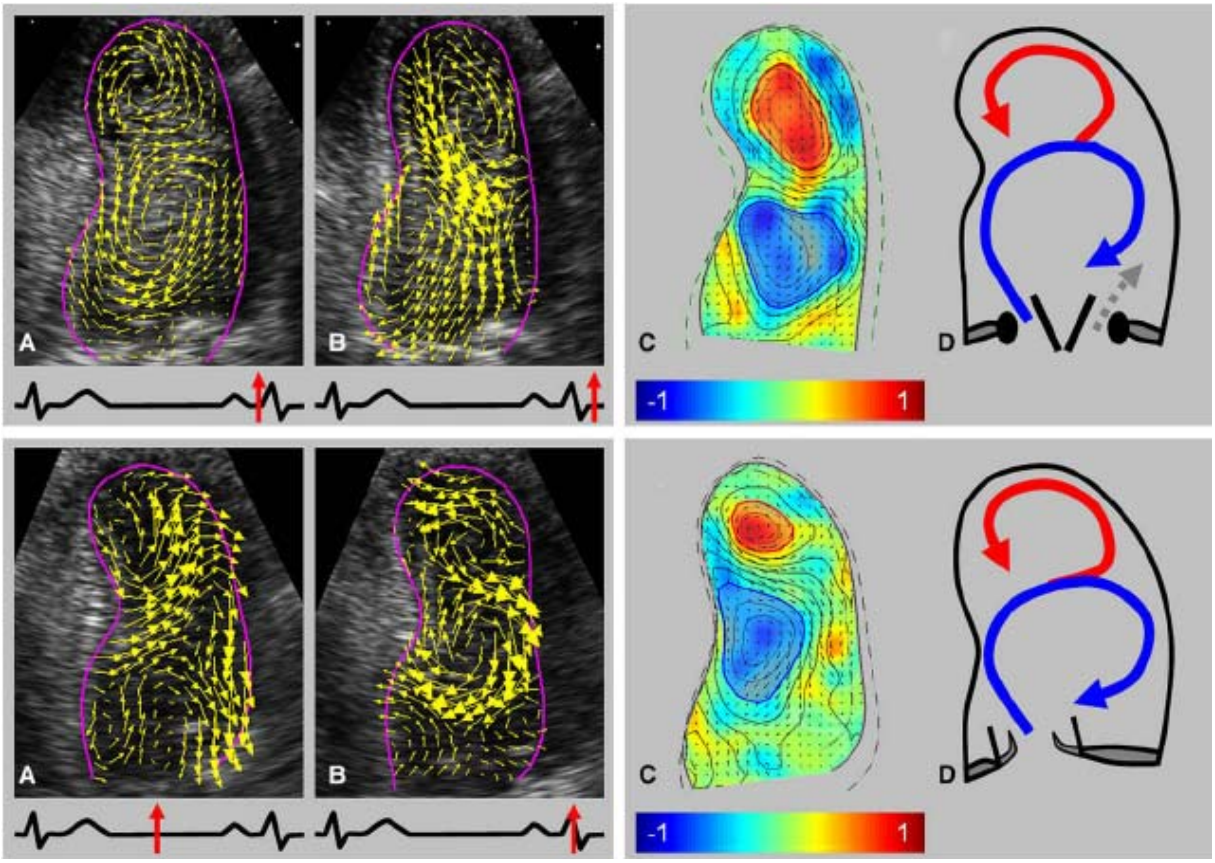

Figure 6. Flow patterns in patients with bi-leaflet valves in anatomic orientation (upper panels) and bioprosthetic valves (lower panels), both with marked midseptal hypertrophy. A and B, see text for detailed description. ECG was used as a time reference. Normalized regional vorticity in the plane of the 4-chamber view is averaged over one cardiac cycle (C). Schematic drawings of the dominating flow path as observed during diastole in the 4-chamber view are shown (D).

5.3.4. Flow patterns of bioprosthetic valves

5.3.4.1. General pattern

The flow through the bioprosthesis generates a central jet directed toward the apex *(Figure 7., A)*. It generates a vortex ring that is visualized as a vortex pair in a 2-dimensional image *(Figure 7., B)*. With atrial contraction, the same flow pattern is reinforced. At the beginning of systole *(Figure 7., C),* the symmetry of the flow pattern is lost, the posterolateral vortex part becomes dominant, and the outflowing blood crosses the previous inflow area again *(Figure 7., D)*. This dominance of the posterolateral vortex part might also be noted in the time-

averaged colour-coded representation of left ventricular vorticity from both apical views *(Figure 7., E and G).*

5.3.4.2. Influence of valve position and left ventricular geometry

One patient had a marked anteroseptal position of the bioprosthesis, resulting in an inflow jet toward the anterior septum. Similar to the abovementioned bi-leaflet valves, this jet is then redirected toward the lateral wall by the hypertrophied midseptum *(Figure 6., A, lower panel)* and forms two vortices *(Figure 6., B, lower panel)*. *Figure 6., C (lower panel)*, shows the time-averaged vorticity in the 4-chamber view, and *Figure 6., D (lower panel)*, provides a schematic drawing of the main flow paths.

In hearts of patients with bioprosthetic valves, parameters of energy dissipation were higher than in hearts of healthy subjects. RS showed a significant difference, and VPC showed a trend (Table 6). Energy dissipation was particularly high in the patient with altered left ventricular geometry (RS: 2.90±0.48; VPC: 1.76±0.66).

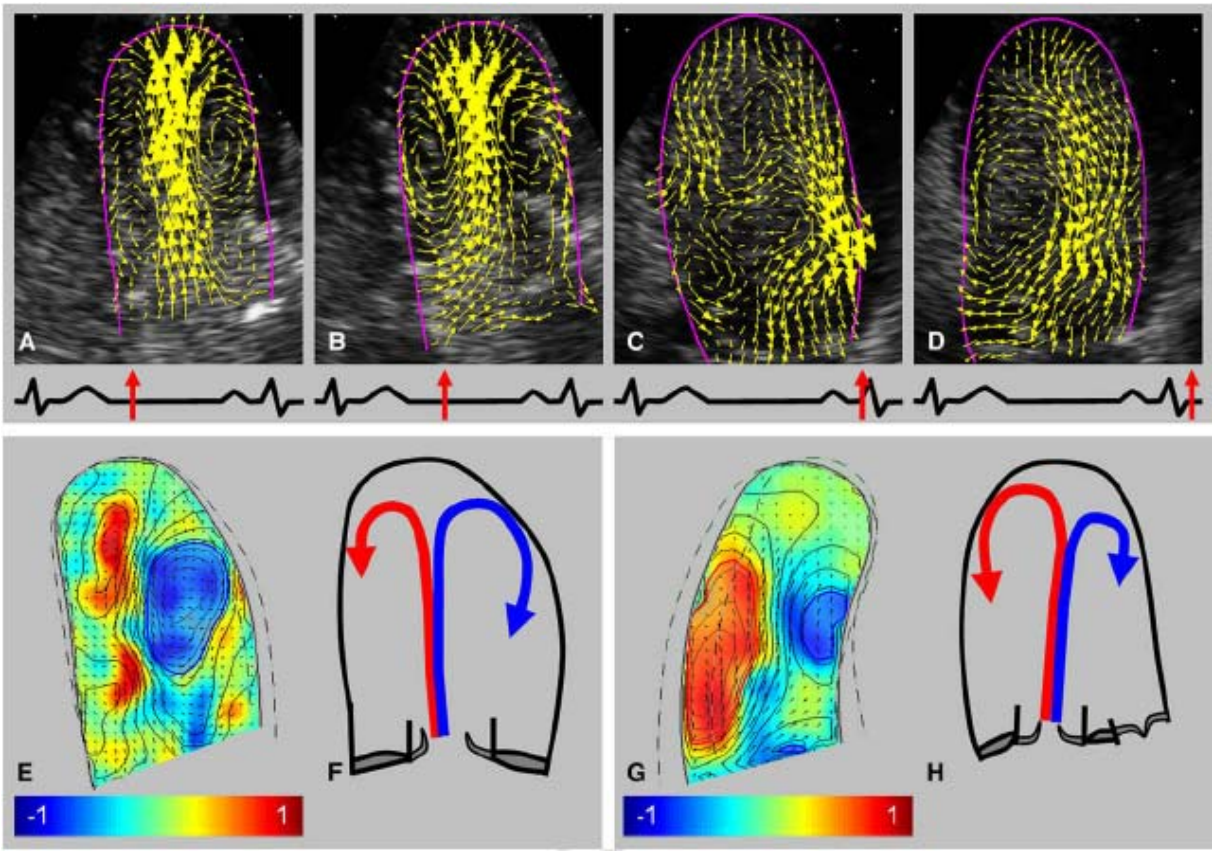

Figure 7. General flow pattern in patients with bioprosthetic valves. There is a similar display as in Figure 5.2. See the text for a detailed description.

5.3.5. Flow pattern of a tilting-disc valve with anterior orientation of the greater orifice

In our patient with a single-disc prosthesis, the majority of the inflow is directed through the greater orifice toward the septum and then redirected by the hypertrophied ventricular septum to form a large, clockwise rotating vortex filling the basal two thirds of the ventricle and a small, counter clockwise rotating vortex in the anterior apex *(Figure 8., A)*. Similar to the other prosthetic valves, the outflowing blood crosses the previous inflow area *(Figure 8., B)*. Likewise, parameters of energy dissipation are higher compared with those seen in healthy hearts (Table 6).

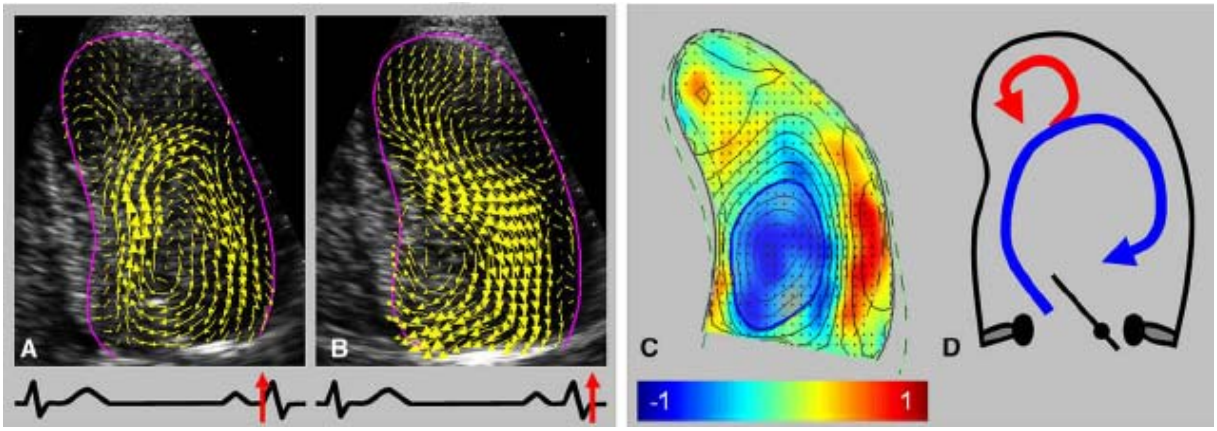

Figure 8. Flow pattern in a patient with a tilting-disc valve with anterior orientation of the greater orifice. This is the same principle of display as in Figure 5.4. See the text for a detailed description.

5.4. Discussion

5.4.1. Flow Patterns in Healthy Hearts

In our study we found vortical flow patterns in the left ventricle, detaching from the mitral valve during mitral inflow *(Figure 4.)*. Based on the 2-dimensional data obtained in the three apical image planes, we could conclude that a 3-dimensional, torus-like vortex structure (similar to a donut or a smoke ring puffed out by a cigarette smoker) enters the left ventricle during the beginning of early diastole. Because of the asymmetry of the left ventricular inflow tract, the anteroseptal side of the vortex formation becomes dominant

Table 6 Characteristics of the left ventricular vortical flow in normal hearts and patients with prosthetic mitral valves

	Healthy hearts	**All prosthetic valves**	**p***	**Bi-leaflet valves**	**p****	**Bioprosthetic valves**	**p****	**Tilting disc valve**	**p****
VA (%)	50.3±5.9	53.5±13.6	0.352	50.6±16.7	1.000	56.9±8.5	1.000	56.2±15.2	1.000
RS	1.62±0.43	2.36±0.71	**0.000**	2.33±0.92	**0.037**	2.43±0.48	**0.034**	2.28±0.16	0.941
VRS	0.43±0.10	0.52±0.16	0.052	0.50±0.16	1.000	0.53±0.18	0.828	0.64±0.09	0.315
VPC	0.72±0.24	1.20±0.51	**0.000**	1.20±0.60	**0.041**	1.22±0.49	0.076	1.22±0.29	0.743

VA – vortex area in % of the left ventricular area. RS, VRS and VPC are parameters of flow pattern dependent energy dissipation in the left ventricle: RS - relative pulsatile vorticity strength; VRS - vortex relative pulsatile vorticity strength; VPC - vortex pulsation correlation. See text for further details. P-values vs. healthy hearts *) t-test, **) ANOVA post hoc test (Bonferroni)

and persists in the centre of the cavity, leading to the described rotational motion of the blood in the ventricle, whereas the smaller posterior part of the vortex diminishes rapidly. This is in concordance with prior physical and numeric modelling [21, 23-24, 70] and supported by in vivo studies with colour Doppler imaging[71] and MRI.[29-30, 63]

During atrial contraction, we found a more laterally directed mitral inflow forming a second vortex structure at the basal half of the ventricle. This is in concordance with MRI observations reported by Fyrenius and colleagues,[63] who similarly describe two different pathways of the inflowing blood during early and late filling. At the very end of diastole, a single large vortex is present, and blood is smoothly redirected toward the outflow tract for the following systole, as predicted based on numeric modelling by others.[23, 70]

5.4.2. Bi-leaflet valve in anatomic orientation

The non-physiologic inflow through a bi-leaflet valve leads to a completely different and more complex flow pattern in the left ventricle *(Figure 5.)*. In most of our patients, the inflow through the septal orifice was dominant and resulted in a major vortex rotating in the opposite direction compared with that seen in healthy hearts. This is partially supported by prior in vitro simulations [22, 72-73]and animal experiments [27, 31, 74]and might be explained by asymmetry of the left ventricular inflow tract. Because the septal inflow chamber, which includes the left ventricular outflow tract, is larger than the posterior one, the mitral inflow penetrates the ventricle mainly through the septal orifice.[27] Asynchronous opening of the leaflets[22] or asymmetry of the atrial flow[20, 64, 73] might further contribute.

Our measurements indicate for the first time, that intracavitary blood flow in patients with bi-leaflet valve prostheses is less energy efficient than in healthy hearts. Higher energy dissipation can be explained by the non-physiologic formation of a major vortex rotating in the opposite direction compared with that seen in healthy hearts and the outflowing blood crossing the inflow tract during systole.

Our results show that unfavourable left ventricular geometry further disturbs vortex formation. This has not been described previously because experimental studies

assume “normal” ventricles. Nevertheless, with the observation of two counterrotating vortices in the apical and basal halves of the ventricle, we can show for the first time a human in vivo correlate to the colour Doppler patterns described by Van Rijk–Zwikker and co-workers[27] in pigs.

5.4.3. Bioprosthetic valve

In concordance with the numeric simulations of Pedrizzetti and Domenichini,[25] we observed in patients with bioprosthetic valves a completely symmetric inflow pattern leading to a symmetric vortex ring *(Figure 7.)*. At the end of diastole, this symmetry is lost, and the part of the vortex ring that becomes dominant rotates in the opposite direction compared with that seen in healthy hearts. Our data indicate that the flow pattern in bioprosthetic valves also results in higher energy dissipation. This might be explained by the division of the blood stream in counterrotating parts that leads to a higher loss of kinetic energy than in the single vortex of a normal heart. Position of the valve and, similar to bi-leaflet prosthesis, left ventricular geometry markedly influence the flow pattern. Our data help us understand the previous colour Doppler observations of Maire and associates,[28] who described unusual flow patterns in patients with an eccentric bioprosthetic valve position.

5.4.4. Tilting-disc valve with anterior orientation of the greater orifice

Our findings in the patient with a tilting-disc prosthesis are in concordance with previous Doppler- or MRI-based publications.[26, 28, 32] The presence of a hypertrophied left ventricular septum explains the formation of the additional counterrotating vortex at the apex *(Figure 8.)*. Single tilting-disc prostheses are rarely used in the mitral position nowadays. Based on our experiences, however, we hypothesize that the normal direction of inflow vortex formation and the separation of inflow and outflow tracts might be best simulated by a mitral tilting-disc prosthesis with the larger orifice in a posterior orientation.[26, 28, 32] To what extent this might counterbalance the disadvantages of this type of valve replacement therapy remains to be determined.

5.4.5. Clinical considerations

It has been assumed based on numeric simulations and in vitro and in vivo experiments, as well as colour Doppler and MRI measurements, that prosthetic heart valves seriously disturb intraventricular flow patterns.[21-22, 25-28, 31-32, 72-74]The application of PIV to echocardiography allows, for the first time, direct visualization and, in part, quantification of those patterns and enables estimation of energy dissipation in the left ventricle by means of a non-invasive technique. Numeric simulations of energy dissipation support the thesis that the natural left ventricle is optimized to forward the blood with the lowest energy loss possible.[68] A discontinuous blood pump can work most efficiently if the momentum of the blood is maintained. A linear arrangement of heart chambers would require constant deceleration and acceleration of the blood and would waste kinetic energy. In contrast to any linear arrangement of heart chambers, it is more energy efficient to have adjacent inflow and outflow tracts and a diastolic vortex formation, which stores energy and redirects the blood stream while maintaining its kinetic energy.[68]

To what extent vortex formation contributes to an optimization of cardiac performance is subject to debate.[75] Some authors assume that accelerating blood accounts only for approximately 2% of the energy consumption of a healthy heart.[76]Pedrizzetti and Domenichini[25] showed in a numeric simulation that even slight changes in mitral valve position can result in changes of energy dissipation in the range of 15%. A counterrotating vortex or more complex flow pattern changes are likely to result in even higher energy loss. It might therefore be relevant to optimize intracavitary blood flow after valve replacement, particularly in dysfunctional ventricles. We believe that this new technique of echocardiographic PIV can contribute to a better understanding of hemodynamic consequences of heart valve surgery and thus to an optimization of such a therapy.

5.4.6. Limitations of the study

The current echocardiographic PIV method is 2-dimensional and thus has limits regarding the analysis of the 3-dimensional structure of flow patterns. This inherent problem of clinical echocardiographic analysis can currently not be solved because of

the low temporal and spatial resolution of echocardiographic 3-dimensional imaging technology. We are confident, however, that merging information from 3 apical views is sufficient to recognize larger 3-dimensional structures in the intracavitary flow of the left ventricle. This is supported by the fact that the results of our data interpretation are in accordance with mathematic modelling and true 3-dimensional MRI measurements of cavitary flow. Future developments in 3-dimensional echocardiography might further improve echocardiographic PIV.

Thus far, flow pattern analysis is descriptive and at best semi-quantitative. The relation between flow patterns and energy dissipation is extremely complex and difficult to express in a few simple, clinically useful numbers. Further studies are needed to better understand these relationships and to offer quantitative measures for intracavitary blood flow analysis.

Ventricular shape changes caused by age, previous mitral valve disease, or removal of the subvalvular apparatus were not considered. The study was not powered to investigate possible relations between valve size and flow patterns. Our data suggest, however, that the presence of a mitral valve prosthesis dominates intracavitary flow pattern developments and is only modulated by left ventricular geometry. Outcome data are needed to evaluate the clinical relevance of our findings.

6. Discussion

6.1. Left atrial size and function are characteristics of chronic left ventricular diastolic dysfunction

BNP and NT-proBNP levels are known to be elevated in patients with HCM and correlate with New York Heart Association functional class, left ventricular outflow tract gradient and maximal left ventricular wall thickness. [77-80] A close correlation between left atrial volume or function and BNP levels has also been reported in HCM patients,[81] the pathophysiologic background of this relationship, however, is not clear.

BNP is released from both the ventricular and atrial myocardium in response to myocyte stretch and transmural pressure load, still, plasma levels of BNP mainly reflect the degree of left ventricular filling pressure. [82] In addition, previous studies have shown a strong association between left atrial volume and left ventricular diastolic function grade.[45-47] These data suggests that the missing link between left atrial function and NT-proBNP level may be the left ventricular diastolic function. At the same time, in our work and in more studies similarly, Doppler-derived parameters of left ventricular diastolic function and filling pressure showed no or very modest correlation with the BNP level.[81, 83] The explanation of this phenomenon may be, that these techniques present only a snapshot view of diastolic function: the pattern would be altered if loading conditions changed.[84]

On the other hand, the increased left atrial pressure in HCM patients with normal left ventricular systolic function and no significant mitral valve disease has been attributed to left ventricular diastolic dysfunction. The left atrial size may increase with the increase of the left atrial pressure, since the left atrium is a thin-walled structure. The left atrium during ventricular diastole is exposed directly to left ventricular pressures since the mitral valve is open. After distension, there is only a little elastic recoil in the left atrium to respond to the fall in pressure, therefore a chronically dilated left atrium does not change in size with transient changes in left atrial pressure. Thus, unlike the Doppler measures of left ventricular diastolic dysfunction, the left atrial size is independent of loading conditions and correlates with the severity and the time

duration of the diastolic dysfunction. Therefore left atrial size may be superior to the Doppler-derived parameters in the characterization of left ventricular diastolic dysfunction and thus it shows a stronger correlation with the BNP levels.

Much less data are available in the literature about the deterioration of A', parallel with the impairment of left ventricular diastolic function.[85] Our data, however, suggest, that the behaviour of the left ventricular size and A' parameter is similar in patients with preserved ejection fraction and diastolic dysfunction, which may explain the correlation we have found between NT-proBNP level and A' parameter in our study.

6.2. Importance of TDI in the assessment of right ventricular function in CTD patients

CTDs are multi-system disorders characterized by extensive involvement of the internal organs. Cardiac involvement occurs very often in these patients, manifesting as pericardial effusion, valve disease or myocardial fibrosis and resulting in heart failure.

PAH is one of the relatively common complications of CTDs, and finally results in right heart failure. The prognosis in these patients correlates with the presence of PAH. Mukerjee et al. suggested that the hemodynamic parameters of right ventricular dysfunction are strong predictors of outcome in CTD patients.[86] Right ventricular function, however, is rarely evaluated. This is because of complex chamber geometry and lack of objective methods. Traditional methods used to assess right ventricular function such as radionuclide ventriculography, magnetic resonance imaging, and the thermodilution method of right heart catheterization are time-consuming and relatively expensive, and can not be used at the bedside.[58]

On the other hand, the development of echocardiography allowed the assessment of the right ventricular systolic and diastolic function non-invasively. Traditionally, right ventricular systolic function was derived mainly from tricuspid annular displacement, while Doppler parameters of the right ventricular filling were used to characterize the diastolic function. Recently, TDI of the tricuspid annulus has been shown to be an accurate and reproducible representation of global right ventricular systolic and diastolic function.[55-56] In addition, both systolic and diastolic functional parameters

represents a very powerful tool for risk stratification of patients with right heart failure.[87]

In our work we described a new application of the early diastolic TDI parameter, proving, that it is a promising screening method to confirm or eliminate suspicion of stress induced pulmonary hypertension in patients with CTD.

6.3. Flow pattern inside the heart: outlook

In our study, for the first time, we presented a description of normal intraventricular blood flow patterns and their changes caused by mitral valve surgery based on non-invasive echocardiographic PIV. The technique was feasible in the clinical setting and allowed clear differentiation of normal from disturbed flow patterns after mitral valve replacement, as well as quantification of left ventricular energy dissipation.

Future applications of echocardiographic PIV might comprise the study of postoperative left ventricular flow characteristics to optimize bioprosthetic and mechanical heart valve design. Preoperative PIV could help to select most optimal implantation techniques, such as valve replacement with or without preservation of the subvalvular apparatus, or to optimize implantation for a specific pathology, such as postinfarction patients or hearts with septal hypertrophy. Flow investigations by PIV could also improve valve reconstruction strategies or help to optimize other surgical cardiovascular interventions, such as Fontan operations. Pathophysiologic knowledge could be gained on the relation between left ventricular and left atrial flow characteristics and the rate of thromboembolic events. Our results suggest, that echocardiographic PIV has potential clinical importance for the analysis of cardiac function and guidance of cardiosurgical interventions.

6.4. Conclusion

Heart failure is an increasing and leading cause of cardiovascular morbidity, hospitalisation and death worldwide. Echocardiography is uniquely suited to characterize anatomical and functional abnormalities in patients at risk of developing heart failure, suspected of having heart failure, and with symptomatic heart failure.

Furthermore, echocardiography can provide prognostic information and assist in the management of patients with acute, chronic and end-stage heart failure.

Traditional methods for assessing cardiac morphology, function and hemodynamics, however, were insufficient to clarify several challenging problems of heart failure patients. Therefore, contemporary imaging techniques in the assessment of heart failure patients are moving toward evaluation of myocardial motion and deformation or intracavitary flow.

In our work we used tissue Doppler imaging and particle image velocimetry to evaluate specific problems in patients with left ventricular diastolic dysfunction, right ventricular dysfunction or prosthetic mitral valves. Our results prove the usefulness of the novel echocardiographic techniques in the solution of specific problems in heart failure patients.

7. Novel findings

7.1. Based on TDI measurement we proved a significant correlation between B-type natriuretic peptide level and the left atrial function in patients with hypertrophic cardiomyopathy.

7.2. By the help of TDI measurements and right heart catheterisation we confirmed the observation, that isolated resting longitudinal diastolic dysfunction of the right ventricle is the sign of exercise induced pulmonary hypertension in patients with connective tissue diseases.

7.3. Our results demonstrated, that the new method of echocardiographic particle image velocimetry is able to describe and distinguish left ventricular flow patterns in healthy hearts and in patients with different types of prosthetic mitral valves.

7.4. By the help of echocardiographic particle image velocimetry we proved, that flow-mediated energy dissipation in the left ventricle is significantly higher in patients with prosthetic mitral valves than in healthy subjects.

8. References

1. Rushmer RF, Crystal DK, Wagner C. The functional anatomy of ventricular contraction. Circ Res 1953;1:162-70.

2. Isaaz K, Thompson A, Ethevenot G, Cloez JL, Brembilla B, Pernot C. Doppler echocardiographic measurement of low velocity motion of the left ventricular posterior wall. Am J Cardiol 1989;64:66-75.

3. Heimdal A, Stoylen A, Torp H, Skjaerpe T. Real-time strain rate imaging of the left ventricle by ultrasound. J Am Soc Echocardiogr 1998;11:1013-9.

4. Leitman M, Lysyansky P, Sidenko S, et al. Two-dimensional strain-a novel software for real-time quantitative echocardiographic assessment of myocardial function. J Am Soc Echocardiogr 2004;17:1021-9.

5. Kheradvar A, Houle H, Pedrizzetti G, et al. Echocardiographic Particle Image Velocimetry: A Novel Technique for Quantification of Left Ventricular Blood Vorticity Pattern. J Am Soc Echocardiogr 2010;23:86-94.

6. Sengupta PP, Khandheria BK, Korinek J, et al. Left ventricular isovolumic flow sequence during sinus and paced rhythms: new insights from use of high-resolution Doppler and ultrasonic digital particle imaging velocimetry. J Am Coll Cardiol 2007;49:899-908.

7. Zheng H, Mukdadi O, Kim HB, Hertzberg J, Shandas R. Advantages in using multi-frequency driving to enhance ultrasound contrast microbubble non-linearities for optimizing echo particle image velocimetry techniques. In; 2004; Arlington, VA; 2004. p. 500-3.

8. Hong GR, Pedrizzetti G, Tonti G, et al. Characterization and quantification of vortex flow in the human left ventricle by contrast echocardiography using vector particle image velocimetry. JACC Cardiovasc Imaging 2008;1:705-17.

9. Yeo KT, Dumont KE, Brough T. Elecsys NT-ProBNP and BNP assays: are there analytically and clinically relevant differences? J Card Fail 2005;11:S84-8.

10. Maisel A. B-type natriuretic peptide levels: a potential novel "white count" for congestive heart failure. J Card Fail 2001;7:183-93.

11. Briguori C, Betocchi S, Manganelli F, et al. Determinants and clinical significance of natriuretic peptides and hypertrophic cardiomyopathy. Eur Heart J 2001;22:1328-36.

12. Mottram PM, Leano R, Marwick TH. Usefulness of B-type natriuretic peptide in hypertensive patients with exertional dyspnea and normal left ventricular ejection fraction and correlation with new echocardiographic indexes of systolic and diastolic function. Am J Cardiol 2003;92:1434-8.

13. Paulus WJ. Natriuretic peptides to probe haemodynamic overload in hypertrophic cardiomyopathy. Eur Heart J 2001;22:1249-51.

14. Simonneau G, Robbins IM, Beghetti M, et al. Updated clinical classification of pulmonary hypertension. J Am Coll Cardiol 2009;54:S43-54.

15. Distler O, Pignone A. Pulmonary arterial hypertension and rheumatic diseases--from diagnosis to treatment. Rheumatology (Oxford) 2006;45 Suppl 4:iv22-5.

16. Claussen M, Riemekasten G, Hoeper MM. [Pulmonary arterial hypertension in collagenoses]. Z Rheumatol 2009;68:630-2, 4-8.

17. Alkotob ML, Soltani P, Sheatt MA, et al. Reduced exercise capacity and stress-induced pulmonary hypertension in patients with scleroderma. Chest 2006;130:176-81.

18. Callejas-Rubio JL, Moreno-Escobar E, de la Fuente PM, et al. Prevalence of exercise pulmonary arterial hypertension in scleroderma. J Rheumatol 2008;35:1812-6.

19. Steen V, Chou M, Shanmugam V, Mathias M, Kuru T, Morrissey R. Exercise-induced pulmonary arterial hypertension in patients with systemic sclerosis. Chest 2008;134:146-51.

20. Kilner PJ, Yang GZ, Wilkes AJ, Mohiaddin RH, Firmin DN, Yacoub MH. Asymmetric redirection of flow through the heart. Nature 2000;404:759-61.

21. Bellhouse BJ. Fluid mechanics of a model mitral valve and left ventricle. Cardiovasc Res 1972;6:199-210.

22. Pierrakos O, Vlachos PP, Telionis DP. Time-resolved DPIV analysis of vortex dynamics in a left ventricular model through bileaflet mechanical and porcine heart valve prostheses. J Biomech Eng 2004;126:714-26.

23. Domenichini F, Pedrizzetti G, Baccani B. Three-dimensional filling flow into a model left ventricle. Journal of Fluid Mechanics 2005;539:179-98.

24. Domenichini F, Querzoli G, Cenedese A, Pedrizzetti G. Combined experimental and numerical analysis of the flow structure into the left ventricle. Journal of Biomechanics 2007;40:1988-94.

25. Pedrizzetti G, Domenichini F. Nature optimizes the swirling flow in the human left ventricle. Phys Rev Lett 2005;95:108101.

26. Pop G, Sutherland GR, Roelandt J, Vletter W, Bos E. What is the ideal orientation of a mitral disc prosthesis? An in vivo haemodynamic study based on colour flow imaging and continuous wave Doppler. Eur Heart J 1989;10:346-53.

27. Van Rijk-Zwikker GL, Delemarre BJ, Huysmans HA. The orientation of the bi-leaflet CarboMedics valve in the mitral position determines left ventricular spatial flow patterns. Eur J Cardiothorac Surg 1996;10:513-20.

28. Maire R, Ikram S, Odemuyiwa O, et al. Abnormalities of left ventricular flow following mitral valve replacement: a colour flow Doppler study. Eur Heart J 1994;15:293-302.

29. Kim WY, Walker PG, Pedersen EM, et al. Left ventricular blood flow patterns in normal subjects: a quantitative analysis by three-dimensional magnetic resonance velocity mapping. J Am Coll Cardiol 1995;26:224-38.

30. Wigstrom L, Ebbers T, Fyrenius A, et al. Particle trace visualization of intracardiac flow using time-resolved 3D phase contrast MRI. Magn Reson Med 1999;41:793-9.

31. Machler H, Perthel M, Reiter G, et al. Influence of bileaflet prosthetic mitral valve orientation on left ventricular flow--an experimental in vivo magnetic resonance imaging study. Eur J Cardiothorac Surg 2004;26:747-53.

32. Machler H, Reiter G, Perthel M, et al. Influence of a tilting prosthetic mitral valve orientation on the left ventricular flow - an experimental in vivo magnetic resonance imaging study. Eur J Cardiothorac Surg 2007;32:102-7.

33. Matsumura Y, Elliott PM, Virdee MS, Sorajja P, Doi Y, McKenna WJ. Left ventricular diastolic function assessed using Doppler tissue imaging in patients with hypertrophic cardiomyopathy: relation to symptoms and exercise capacity. Heart 2002;87:247-51.

34. Lengyel M, Nagy A, Zorandi A. [Tissue Doppler echocardiography: a new technique to assess diastolic function]. Orv Hetil 2002;143:333-9.

35. Sohn DW, Chai IH, Lee DJ, et al. Assessment of mitral annulus velocity by Doppler tissue imaging in the evaluation of left ventricular diastolic function. J Am Coll Cardiol 1997;30:474-80.

36. Hesse B, Schuele SU, Thamilasaran M, Thomas J, Rodriguez L. A rapid method to quantify left atrial contractile function: Doppler tissue imaging of the mitral annulus during atrial systole. Eur J Echocardiogr 2004;5:86-92.

37. Khankirawatana B, Khankirawatana S, Peterson B, Mahrous H, Porter TR. Peak atrial systolic mitral annular velocity by Doppler tissue reliably predicts left atrial systolic function. J Am Soc Echocardiogr 2004;17:353-60.

38. Sengupta PP, Mohan JC, Pandian NG. Tissue Doppler echocardiography: principles and applications. Indian Heart J 2002;54:368-78.

39. Nagueh SF, Middleton KJ, Kopelen HA, Zoghbi WA, Quinones MA. Doppler tissue imaging: a noninvasive technique for evaluation of left ventricular relaxation and estimation of filling pressures. J Am Coll Cardiol 1997;30:1527-33.

40. Ommen SR, Nishimura RA, Appleton CP, et al. Clinical utility of Doppler echocardiography and tissue Doppler imaging in the estimation of left ventricular filling pressures: A comparative simultaneous Doppler-catheterization study. Circulation 2000;102:1788-94.

41. Collinson PO, Barnes SC, Gaze DC, Galasko G, Lahiri A, Senior R. Analytical performance of the N terminal pro B type natriuretic peptide (NT-proBNP) assay on the Elecsys 1010 and 2010 analysers. Eur J Heart Fail 2004;6:365-8.

42. Nagueh SF, Lakkis NM, Middleton KJ, Spencer WH, 3rd, Zoghbi WA, Quinones MA. Doppler estimation of left ventricular filling pressures in patients with hypertrophic cardiomyopathy. Circulation 1999;99:254-61.

43. Matsuda Y, Toma Y, Ogawa H, et al. Importance of left atrial function in patients with myocardial infarction. Circulation 1983;67:566-71.

44. Greenberg B, Chatterjee K, Parmley WW, Werner JA, Holly AN. The influence of left ventricular filling pressure on atrial contribution to cardiac output. Am Heart J 1979;98:742-51.

45. Matsuda M, Matsuda Y. Mechanism of left atrial enlargement related to ventricular diastolic impairment in hypertension. Clin Cardiol 1996;19:954-9.

46. Tsang TS, Barnes ME, Gersh BJ, Bailey KR, Seward JB. Left atrial volume as a morphophysiologic expression of left ventricular diastolic dysfunction and relation to cardiovascular risk burden. Am J Cardiol 2002;90:1284-9.

47. Pritchett AM, Mahoney DW, Jacobsen SJ, Rodeheffer RJ, Karon BL, Redfield MM. Diastolic dysfunction and left atrial volume: a population-based study. J Am Coll Cardiol 2005;45:87-92.

48. Payne RM, Stone HL, Engelken EJ. Atrial function during volume loading. J Appl Physiol 1971;31:326-31.

49. Prioli A, Marino P, Lanzoni L, Zardini P. Increasing degrees of left ventricular filling impairment modulate left atrial function in humans. Am J Cardiol 1998;82:756-61.

50. Teo SG, Yang H, Chai P, Yeo TC. Impact of left ventricular diastolic dysfunction on left atrial volume and function: a volumetric analysis. Eur J Echocardiogr 2010;11:38-43.

51. Badesch DB, Champion HC, Sanchez MA, et al. Diagnosis and assessment of pulmonary arterial hypertension. J Am Coll Cardiol 2009;54:S55-66.

52. Lindqvist P, Caidahl K, Neuman-Andersen G, et al. Disturbed right ventricular diastolic function in patients with systemic sclerosis: a Doppler tissue imaging study. Chest 2005;128:755-63.

53. Huez S, Roufosse F, Vachiery JL, et al. Isolated right ventricular dysfunction in systemic sclerosis: latent pulmonary hypertension? Eur Respir J 2007;30:928-36.

54. Meune C, Avouac J, Wahbi K, et al. Cardiac involvement in systemic sclerosis assessed by tissue-doppler echocardiography during routine care: A controlled study of 100 consecutive patients. Arthritis Rheum 2008;58:1803-9.

55. Meluzin J, Spinarova L, Bakala J, et al. Pulsed Doppler tissue imaging of the velocity of tricuspid annular systolic motion; a new, rapid, and non-invasive method of evaluating right ventricular systolic function. Eur Heart J 2001;22:340-8.

56. Alam M, Wardell J, Andersson E, Samad BA, Nordlander R. Characteristics of mitral and tricuspid annular velocities determined by pulsed wave Doppler tissue imaging in healthy subjects. J Am Soc Echocardiogr 1999;12:618-28.

57. Ruan Q, Nagueh SF. Clinical application of tissue Doppler imaging in patients with idiopathic pulmonary hypertension. Chest 2007;131:395-401.

58. Hsiao SH, Lee CY, Chang SM, Lin SK, Liu CP. Right heart function in scleroderma: insights from myocardial Doppler tissue imaging. J Am Soc Echocardiogr 2006;19:507-14.

59. Milo S, Rambod E, Gutfinger C, Gharib M. Mitral mechanical heart valves: in vitro studies of their closure, vortex and microbubble formation with possible medical implications. Eur J Cardiothorac Surg 2003;24:364-70.

60. Cen YY, Glower DD, Landolfo K, et al. Comparison of survival after mitral valve replacement with biologic and mechanical valves in 1139 patients. J Thorac Cardiovasc Surg 2001;122:569-77.

61. Rahimtoola SH. Choice of prosthetic heart valve for adult patients. J Am Coll Cardiol 2003;41:893-904.

62. Gharib M, Kremers D, Koochesfahani M, Kemp M. Leonardo's vision of flow visualization. Experiments in Fluids 2002;33:219-23.

63. Fyrenius A, Wigstrom L, Bolger AF, et al. Pitfalls in Doppler evaluation of diastolic function: insights from 3-dimensional magnetic resonance imaging. J Am Soc Echocardiogr 1999;12:817-26.

64. Fyrenius A, Wigstrom L, Ebbers T, Karlsson M, Engvall J, Bolger AF. Three dimensional flow in the human left atrium. Heart 2001;86:448-55.

65. Yang GZ, Mohiaddin RH, Kilner PJ, Firmin DN. Vortical flow feature recognition: a topological study of in vivo flow patterns using MR velocity mapping. J Comput Assist Tomogr 1998;22:577-86.

66. Kvitting JP, Ebbers T, Wigstrom L, Engvall J, Olin CL, Bolger AF. Flow patterns in the aortic root and the aorta studied with time-resolved, 3-dimensional, phase-contrast magnetic resonance imaging: implications for aortic valve-sparing surgery. J Thorac Cardiovasc Surg 2004;127:1602-7.

67. Batchelor G. The theory of homogeneous turbulence. Cambridge (UK): Cambridge University Press; 1953.

68. Krueger PS, Gharib M. The significance of vortex ring formation to the impulse and thrust of a starting jet. Physics of Fluids 2003;15:1271-81.

69. Adrian RJ. Particle-imaging techniques for experimental fluid mechanics. Annual Review of Fluid Mechanics 1991;23:261-304.

70. Bolzon G, Zovatto L, Pedrizzetti G. Birth of three-dimensionality in a pulsed jet through a circular orifice. Journal of Fluid Mechanics 2003:209-18.

71. Rodevand O, Bjornerheim R, Edvardsen T, Smiseth OA, Ihlen H. Diastolic flow pattern in the normal left ventricle. J Am Soc Echocardiogr 1999;12:500-7.

72. Schoephoerster RT, Chandran KB. Velocity and turbulence measurements past mitral valve prostheses in a model left ventricle. J Biomech 1991;24:549-62.

73. Garitey V, Gandelheid T, Fuseri J, Pelissier R, Rieu R. Ventricular flow dynamic past bileaflet prosthetic heart valves. Int J Artif Organs 1995;18:380-91.

74. Jones M, Eidbo EE. Doppler color flow evaluation of prosthetic mitral valves: experimental epicardial studies. J Am Coll Cardiol 1989;13:234-40.

75. Watanabe H, Sugiura S, Hisada T. The looped heart does not save energy by maintaining the momentum of blood flowing in the ventricle. Am J Physiol Heart Circ Physiol 2008;294:H2191-6.

76. Schmidt R, Lang F, Thews G. Physiologie des Menschen mit Pathophysiologie. Heidelberg: Springer; 2004.

77. Arteaga E, Araujo AQ, Buck P, Ianni BM, Rabello R, Mady C. Plasma amino-terminal pro-B-type natriuretic peptide quantification in hypertrophic cardiomyopathy. Am Heart J 2005;150:1228-32.

78. Maron BJ, Tholakanahalli VN, Zenovich AG, et al. Usefulness of B-type natriuretic peptide assay in the assessment of symptomatic state in hypertrophic cardiomyopathy. Circulation 2004;109:984-9.

79. Mutlu B, Bayrak F, Kahveci G, Degertekin M, Eroglu E, Basaran Y. Usefulness of N-terminal pro-B-type natriuretic peptide to predict clinical course in patients with hypertrophic cardiomyopathy. Am J Cardiol 2006;98:1504-6.

80. Yoshibayashi M, Kamiya T, Saito Y, Matsuo H. Increased plasma levels of brain natriuretic peptide in hypertrophic cardiomyopathy. N Engl J Med 1993;329:433-4.

81. Kahveci G, Bayrak F, Mutlu B, Basaran Y. Determinants of elevated NT-proBNP levels in patients with hypertrophic cardiomyopathy: an echocardiographic study. Heart Lung Circ 2009;18:266-70.

82. Yoshimura M, Yasue H, Okumura K, et al. Different secretion patterns of atrial natriuretic peptide and brain natriuretic peptide in patients with congestive heart failure. Circulation 1993;87:464-9.

83. Geske JB, Sorajja P, Nishimura RA, Ommen SR. Evaluation of left ventricular filling pressures by Doppler echocardiography in patients with hypertrophic cardiomyopathy: correlation with direct left atrial pressure measurement at cardiac catheterization. Circulation 2007;116:2702-8.

84. Douglas PS. The left atrium: a biomarker of chronic diastolic dysfunction and cardiovascular disease risk. J Am Coll Cardiol 2003;42:1206-7.

85. Poh KK, Chan MY, Yang H, Yong QW, Chan YH, Ling LH. Prognostication of valvular aortic stenosis using tissue Doppler echocardiography: underappreciated importance of late diastolic mitral annular velocity. J Am Soc Echocardiogr 2008;21:475-81.

86. Mukerjee D, St George D, Coleiro B, et al. Prevalence and outcome in systemic sclerosis associated pulmonary arterial hypertension: application of a registry approach. Ann Rheum Dis 2003;62:1088-93.

87. Meluzin J, Spinarova L, Hude P, et al. Prognostic importance of various echocardiographic right ventricular functional parameters in patients with symptomatic heart failure. J Am Soc Echocardiogr 2005;18:435-44.

9. Publications of the author

10.1. Original papers and letters

10.1.1. In connection with the topic of the thesis

Faludi R., Tóth L., Pótó L., Cziráki A., Simor T., Papp L.: A B típusú natriuretikus peptid (NT-proBNP) szint és a diastolés funkciót jellemző hagyományos és szöveti Doppler-echokardiográfiás paraméterek kapcsolata hypertrophiás cardiomyopathiában szenvedő betegekben. Orvosi Hetilap 2005;146:23-26.

Faludi R., Komócsi A., Bozó J., Kumánovics G., Czirják L., Papp L., Simor T.: Isolated diastolic dysfunction of right ventricle: stress induced pulmonary hypertension. (Letter to editor) European Respiratory Journal 2008;31:475-6.

IF: 5.545

R. Faludi, M. Szulik, J. D'hooge, P. Herijgers, F. Rademakers, G. Pedrizzetti, J. U. Voigt: Left ventricular flow patterns in healthy subjects and patients with prosthetic mitral valves. An in-vivo-study using Echocardiographic Particle Image Velocimetry. Journal of Thoracic and Cardiovascular Surgery 2010;139:1501-10. **IF≈3.037**

10.1.2. Not in connection with the topic of the thesis

Faludi R., Molnár L., A. Tavakoli, Wéber Gy., László T., Mezőfi Beáta: A distalis ileum arteriovenosus malformatioja által okozott vashiányos anaemia. Orvosi Hetilap 1998;139:125-127.

Faludi R., Horváth I., Végh M., Trompos K., Lovász M., Cziráki A.: A 24 órás vérnyomás monitorozással szinkron EKG-elemzés jelentősége esszenciális hipertóniás betegekben. Granum 2005;8:33-35.

R. Faludi, L. Tóth: Letter to the Editor. American Heart Journal 2006;152:e13.

IF: 3.552

Faludi R., Tóth L., Komócsi A., Varga-Szemes A., Papp L., Simor T.: Chronic postinfarction pseudo-pseudoaneurysm diagnosed by cardiac MRI. Journal of Magnetic Resonance Imaging 2007;26:1656-1658. **IF: 2.209**

Faludi R., Komócsi A.: Pulmonalis hypertonia: gyanú, diagnózis, kezelés. Tüdőgyógyászat 2008;2:27-34.

B. Bódis, O. Karádi, O. M. E. Abdel-Salam, **R. Faludi**, L. Nagy, Gy. Mózsik: Organoprotection and cytoprotection of histamine differ in rats. Inflammopharmacology 1997; 5: 29-41.

Cziráki A., Horváth I., **Faludi R.**: Cilazapril-terápia hatása a vérnyomásra és a hemodinamikai paraméterekre essentialis hypertoniás betegekben. Magyar Belorvosi Archivum 1999; 52: 81-86.

Komócsi A., **Faludi R.**: Pulmonális artériás hypertensio. Focus Medicinae 2007;9:15-18.

Mánfai B., **Faludi R.**, Rausch P., Bozó J., Tahin T., Fődi E., Papp L., Simor T.: Bal pitvari reverz-remodelling pitvarfibrilláció rádiófrekvenciás ablációja után. Cardiologia Hungarica 2009;39:113-117.

Komócsi A., Pintér T., **Faludi R.**, Magyari B., Bozó J., Kumánovics G., Minier T., Radics J., Czirják L.: Overlap of coronary disease and pulmonary arterial hypertension in systemic sclerosis. Annals of the Rheumatic Diseases 2010;69:202-5. **IF≈7.188**

10.2. Citable abstracts

10.2.1. In connection with the topic of the thesis

R. Faludi, L. Tóth, A. Cziráki, I. Repa, L. Papp, T. Simor: Comparative study of left ventricular diastolic function using pulsed tissue Doppler and cardiac MR in patients with hypertrophic cardiomyopathy. European Journal of Echocardiography (Suppl.) 2003;4:61.

R. Faludi, L. Tóth, L. Pótó, A. Cziráki, T. Simor, L. Papp: Relationship between B-type natriuretic peptide levels, conventional Doppler and tissue Doppler echocardiographic parameters in patients with hypertrophic cardiomyopathy. European Journal of Echocardiography (Suppl.) 2004;5:S8.

R. Faludi, L. Tóth, T. Simor, L. Papp: NT-proBNP levels and left atrial volumes in patients with isolated left ventricular diastolic dysfunction. European Journal of Heart Failure (Suppl.), 2005;4:52.

R. Faludi, L. Tóth, E. Fődi, Gy. Költő, B. Gyömörei, T. Simor, L. Papp: Correlation between left ventricular mass and the parameters characterizing the left ventricular diastolic function in patients with hypertrophic cardiomyopathy. European Journal of Echocardiography (Suppl.) 2005;6:S107.

R. Faludi, L. Tóth, Gy. Költő, B. Gyömörei, T. Simor, L. Papp: Assessment of diastolic function using tissue Doppler echocardiography: what is the normal value of the mitral annular early diastolic velocity (Ea)? European Journal of Echocardiography (Suppl.) 2005;6:S179.

R. Faludi, L. Tóth, E. Fődi, Gy. Költő, B. Gyömörei, T. Simor, L. Papp: Correlation between longitudinal systolic function of the left ventricle and the “non-velocity-type” parameters characterizing left ventricular diastolic function. European Journal of Heart Failure (Suppl.) 2006;5:61.

R. Faludi, J. Bozó, A. Komócsi, T. Pintér, G. Kumánovics, L. Czirják, T. Simor, L. Papp: Estimation of pulmonary artery pressure by pulsed wave tissue Doppler imaging of the tricuspid and mitral annulus. European Journal of Echocardiography (Suppl.) 2006;7:S202.

R. Faludi, L. Tóth, E. Fődi, T. Simor and L. Papp: Main determinants of left atrial volume in patients suffering from hypertrophic and dilated cardiomyopathy. European Journal of Heart Failure (Suppl.) 2007;6:S155.

R. Faludi, B. Mánfai, E. Fődi, J. Bozó L. Tóth, P. Cziráki, L. Papp, T. Simor: 2D echocardiographic assessment of left atrial volume: validation by contrast enhanced MRI and CT angiography. European Journal of Echocardiography (Suppl.) 2007; 8:S40.

R. Faludi, M. Szulik, J. D'hooge, F. Rademakers, F. Van De Werf, G. Pedrizzetti, J.U. Voigt: Particle image velocimetry distinguishes pathologic and physiologic LV flow patterns in patients with infarcts and healthy subjects. European Heart Journal (Abstract Supplement) 2008;29:875. **IF: 8.917**

R. Faludi, A. Komócsi, J. Bozó, G. Kumánovics, L. Czirják, L. Papp, T. Simor: Right ventricular dysfunction in patients with resting or stress induced pulmonary arterial hypertension secondary to connective tissue diseases. European Journal of Echocardiography (Suppl.) 2008;9:S53.

R. Faludi, M. Szulik, J. D'hooge, F. Rademakers, F. Van De Werf, P Herijgers, G. Pedrizzetti, J.U. Voigt: Particle Image Velocimetry to assess left ventricular flow patterns in healthy subjects and patients with prosthetic mitral valve. European Journal of Echocardiography (Suppl.) 2008;9:S16.

R. Faludi, M. Szulik, J. D'hooge, F. Rademakers, F. Van De Werf, G. Pedrizzetti, J.U. Voigt: Particle image velocimetry distinguishes pathologic and physiologic LV flow

patterns in patients with infarcts and healthy subjects. European Journal of Echocardiography (Suppl.) 2008;9:S24.

R. Faludi, M. Szulik, J. D'hooge, F. Rademakers, F. Van De Werf, G. Pedrizzetti, J.U. Voigt: Echo particle image velocimetry: A new tool to assess intracavitary flow patterns. European Journal of Echocardiography (Suppl.) 2008;9:S16.

R. Faludi, A. Walker, G. Pedrizzetti, J. Engvall, J.U. Voigt: Can feature tracking correctly detect motion patterns as they occur in blood inside heart chambers? Validation of Echocardiographic Particle Image Velocimetry using moving phantoms. European Heart Journal (Abstract Supplement) 2009;30:350. **IF≈8.917**

R. Faludi, L. Tóth, Á. Varga-Szemes, E. Fődi, T. Simor.: Correlations between systolic and diastolic function in a group of subjects with variable degrees of left ventricular diastolic and systolic dysfunction. European Journal of Heart Failure (Suppl.) 2009;8:1456.

M. Szulik, **R. Faludi**, J. D'hooge, F. Van De Werf, F. Rademakers, R. Willems, T. Kukulski, J.U. Voigt: Apical Transversal Motion - a new integrative approach to predict CRT response. European Heart Journal (Abstract Supplement) 2008;29:5.

IF: 8.917

M. Szulik, J. Stabryla-Deska, **R. Faludi**, R. Willems, T. Kukulski, J.U. Voigt: Rocking heart or rocking apex? Where to analyze dyssynchrony? European Journal of Echocardiography (Suppl.) 2008;9:S101.

M. Szulik, **R. Faludi**, R. Willems, T. Kukulski, J.U. Voigt: Apical transversal motion: a new approach to assess left ventricular dyssynchrony in cardiac resynchronization therapy candidates. European Journal of Echocardiography (Suppl.) 2008;9:S151.

B. Mánfai, **R. Faludi**, E. Fődi, P. Rausch, T. Simor: Assessment of left atrial geometry and function prior to and after catheter ablation of atrial fibrillation. Europace Journal 2009;11: S6. (Abstract 386)

E. Gürel, K. Hristova, M. Szulik, **R. Faludi**, L. Van Casteren, R. Willems, J. D'Hooge, F. Rademakers, J.U. Voigt: The impact of function-flow interaction on left ventricular efficiency - a particle image velocimetry study. European Heart Journal (Abstract Supplement) 2009;30:50. **IF≈8,917**

E. Gürel, K. Hristova, M. Szulik, **R. Faludi**, J. D'Hooge, F. Rademakers, J.U. Voigt: Echocardiographic particle image velocimetry for the detailed analysis of left ventricular flow patterns. European Heart Journal (Abstract Supplement) 2009;30:51. **IF≈8,917**

Faludi R., Tóth L., Cziráki A.: A diastoles dysfunctio vizsgálatának új lehetőségei hypertrophiás cardiomyopathiás betegekben. Magyar Belorvosi Archivum (Suppl.) 2003;56:48.

Faludi R., Tóth L., Pótó L., Cziráki A., Simor T., Papp L.: A B-típusú nátriureticus peptid szint és a szöveti Doppler echocardiográfiás paraméterek kapcsolata hypertrophiás cardiomyopathiás betegekben. Cardiologia Hungarica (Suppl.) 2004;34:C41.

Faludi R., Tóth L., Simor T., Papp L.: NT-proBNP szint és bal pitvari volumenek izolált bal kamrai diastolés funkciózavar esetében. Cardiologia Hungarica (Suppl.) 2005;35:A84.

Faludi R., Tóth L., Fődi E., Gyömörei B., Költő Gy., Simor T., Papp L.: Mely tényezők határozzák meg a bal pitvari volument hipertrófiás és dilatatív cardiomyopathiás betegekben? Cardiologia Hungarica (Suppl.) 2006;36:A82.

Faludi R., Szokodi I., Tóth L., H. Ruskoaho, O. Vuolteenaho, Papp L., Simor T.: Mely tényezők határozzák meg a nátriuretikus peptidek szintjét hipertrófiás és dilatatív cardiomyopathiás betegekben? Cardiologia Hungarica (Suppl.) 2007;37:A9.

Faludi R., M. Szulik, J. D'hooge, F. Rademakers, P. Herijgers, G. Pedrizzetti, J.U. Voigt: Bal kamrai áramlási mintázatok egészségesekben és mitrális műbillentyű-beültetést követően. Cardiologia Hungarica (Suppl.) 2009;39:A16.

Mánfai B., **Faludi R**., Rausch P., Tahin T., Fődi E., Tóth L., Varga-Szemes Á., Papp L., Simor T.: A bal pitvar reverz-remodellációja pitvarfibrilláció radiofrekvenciás ablációja után. Cardiologia Hungarica (Suppl.) 2008;38:B43.

Mánfai B., **Faludi R.**, Rausch P., Tahin T., Fődi E., Papp L., Simor T.: A bal pitvari geometria és funkció vizsgálata pitvarfibrilláció radiofrekvenciás ablációja után. Cardiologia Hungarica (Suppl.) 2008;38:G4.

10.2.2. Not in connection with the topic of the thesis

R. Faludi, L. Molnár, A. Tavakoli, Gy. Wéber, T. László, B. Mezőfi: Arteriovenous malformation of the gastrointestinal tract: an analysis of a case and a review of the literature. Zeitschrift für Gastroenterologie 1998; 36: 421. **IF: 0.896**

Cziráki A., Horváth I., **Faludi R.**: Prevention of nitrate tolerance with angiotensin converting enzyme inhibitors. Perfusion 2000;13:356. **IF: 0.167**

L. Tóth, T. Simor, **R. Faludi**, R. Sepp, I. Repa, L. Papp: Characterization of hypertrophic obstructive and non-obstructive cardiomyopathy using contrast agent enhanced cardiac MRI. Journal of Cardiovascular Magnetic Resonance 2004;6:298-299. **IF: 1.898**

T. Simor, L. Tóth, **R. Faludi**, L. Papp, I. Repa: Characterization of regional function in HCM using contrast agent enhanced cardiac MRI. Journal of Cardiovascular Magnetic Resonance 2004;6:301-302. **IF: 1.898**

L. Tóth, **R. Faludi**, T. Simor, L. Papp: Non compaction cardiomyopathy, family report. European Journal of Echocardiography (Suppl.) 2004;5:S15.

J. Bozó, **R. Faludi**, G. Kumánovics, L. Czirják, A. Cziráki, T. Simor, L. Papp: Arterial stiffness and diastolic dysfunction in patients with systemic sclerosis. European Journal of Echocardiography (Suppl.) 2006;7:S33.

L.Tóth, **R. Faludi**, E. Fődi, M. Knausz, Á. Varga-Szemes, L. Papp, T. Simor: Evidence based, MRI strengthened risk stratification strategy for hypertrophic cardiomyopathy patients - A follow up study. European Journal of Echocardiography (Suppl.) 2006;7:S205.

L. Tóth, **R. Faludi**, A. Tóth, Á. Varga-Szemes, I. Repa, L. Papp and T. Simor: Correlation of the extent of left ventricular noncompaction and left ventricular function. A MRI study. European Journal of Heart Failure (Suppl.) 2007;6:S161.

L.Tóth, Á. Varga-Szemes, **R. Faludi**, R. Sepp, V. Nagy, I. Repa, A. Varga, T. Forster, L. Papp, T. Simor: Which are determinant factors altering left ventricular function and clinical outcome of patients with isolated non compact cardiomyopathy? European Journal of Echocardiography (Suppl.) 2007;8:S165.

Á. Varga-Szemes, L. Tóth, **R. Faludi**, L. Papp, T. Simor: Assessment of regional left ventricular function in isolated left ventricular noncompaction. European Journal of Heart Failure (Suppl.) 2008;7:33.

L. Tóth, Á. Varga-Szemes, **R. Faludi**, A. Tóth, L. Papp, T. Simor: MRI study in isolated left ventricular noncompaction. Journal of Cardiovascular Magnetic Resonance 2007;9:406. **IF: 1.867**

Á. Varga-Szemes, L. Tóth, **R. Faludi**, L. Papp, T. Simor: Assessment of ECG abnormalities in patients with left ventricular noncompaction. European Journal of Echocardiography (Suppl.) 2008;9:S96.

Faludi R., Molnár L., Afshin T., Wéber Gy., László T., Mezőfi B.: A distalis ileum arteriovenosus malformatioja által okozott vashiányos anaemia. Magyar Belorvosi Archivum (Suppl.) 1996;49:57.

Faludi R., Cziráki A., Horváth I., Végh M., Trompos K., Lovász M.: A 24 órás vérnyomás monitorozással szinkron EKG-elemzés jelentősége esszenciális hipertóniás betegekben. Cardiologia Hungarica (Suppl.) 1998;28:41.

Faludi R., Sárszegi Zs., Keller J., Ajtay Z., Goják I., Cziráki A., Papp L.: Ergometria során magas rizikójúnak ítélt betegeknél alkalmazott új therápiás stratégia. Magyar Belorvosi Archivum (Suppl.) 2002;55:59.

Faludi R., Tóth L., Cziráki A., Simor T., Papp L.: Non-compact cardiomyopathia: Esetismertetés és irodalmi áttekintés. Magyar Belorvosi Archivum (Suppl.) 2004;57:47.

Cziráki A., Horváth I., **Faludi R.,** J.D. Catravas: A pulmonalis kapillárisendothelhez kötött angiotenzinkonvertáló enzim aktivitásának meghatározása betegekben. Magyar Belorvosi Archivum (Suppl.) 1998;51:218.

Cziráki A., Horváth I., **Faludi R.**: A pulmonalis és koronáriaendothel-funkció monitorozási lehetőségei betegekben. Magyar Belorvosi Archivum (Suppl.) 1999;52:18.

Cziráki A., Horváth I., **Faludi R.**: Angiotensin konvertáló enzim inhibitorok hatása a nitrát toleranciára iszkémiás szívbetegekben. Cardiologia Hungarica (Suppl.) 2000;30:59.

Cziráki A., Csonka D., **Faludi R.**, Nyárfás G., Sárszegi Zs., Papp L.: A kilélegzett nitrogén monoxid vizsgálata ischaemias szívbetegekben. Cardiologia Hungarica (Suppl.) 2001;31:64.

Cziráki A., Csonka D., **Faludi R.**, Nyárfás G., Sárszegi Zs., Papp L.: A kilélegzett nitrogén monoxid vizsgálata ischaemias szívbetegekben. Magyar Belorvosi Archivum (Suppl.) 2002;55:39.

Király Á., **Faludi R.,** Hunyady B., Illés A., Késmárky G., Radnai B., Undi S., Nagy L.: A nyelőcsőmotilitás változása non-cardiac chest pain (NCCP) betegekben. Magyar Belorvosi Archivum (Suppl.) 2004;57:75.

Tóth L., **Faludi R.**, Knausz M., Simor T., Papp L.: Nonkompakt kardiomiopátia, családleírás, irodalmi áttekintés. Cardiologia Hungarica (Suppl.) 2005;35:A86.

Tóth L., **Faludi R.**, Fődi E., Knausz M., Repa I., Papp L., Simor T.: A szív-MR vizsgálat jelentősége a hirtelen halál rizikójának felmérésében hipertrófiás kardiomiopátiás betegekben. Cardiologia Hungarica (Suppl.) 2006;36:A88.

Bozó J., **Faludi R.**, Tóth L., Simor T., Cziráki A., Kumánovics G., Czirják L., Papp L.: Myocarditis kialakulása scleroderma-myositis overlap szindrómában. Cardiologia Hungarica (Suppl.) 2006;36:A61.

Miklán D., Tóth L., **Faludi R.**, Bozó J., Czirják L., Cziráki A., Papp L., Simor T., Pintér Ö.: Iszkémiás szívbetegség előfordulása Takayasu-arteritises betegeinkben. Cardiologia Hungarica (Suppl.) 2006;36:A73.

Fődi E., **Faludi R**., Rausch P., Tahin T., Tóth A., Tóth L., Simor T., Papp L.: Összehasonlító bal pitvari volumen mérések 3D MR és CT-angiográfia valamint 2D-echokardiográfia alapján. Cardiologia Hungarica (Suppl.) 2006;36:D5.

Varga-Szemes Á., Tóth L., **Faludi R.**, Tóth A., Repa I., Papp L., Simor T.: Szív MR-vizsgálat izolált bal kamrai nonkompakt cardiomyopathiás betegeken. Cardiologia Hungarica (Suppl.) 2007;37:A72.

Varga-Szemes Á., Tóth L., **Faludi R**., Papp L., Simor T.: EKG-eltérések vizsgálata nonkompakt cardiomyopathiás betegeken. Cardiologia Hungarica (Suppl.) 2007;37:C3.

Varga-Szemes Á., Tóth L., **Faludi R.**, Papp L., Simor T.: A regionális bal kamra funkció vizsgálata izolált bal kamrai nonkompaktációban. Cardiologia Hungarica (Suppl.) 2008;38:B7.

Mánfai B., **Faludi R.**, Fődi E., Rausch P., Bozó J., Tóth L., Cziráki P., Simor T.: Alkalmas-e a 2D echocardiográfiás Simpson-módszer a bal pitvar térfogatának mérésére? A módszer validálása MR- és CT-angiográfia segítségével. Cardiologia Hungarica (Suppl.) 2009;39:A24.

Impact factor of original papers: 17.979

Impact factor of citable abstracts: 51.311

9.3. Lectures at international scientific congresses

R. Faludi: A"mobile" source of systemic embolism. EUROECHO Congress, Prague, 2006.

R. Faludi: Tracking cardiac blood flow: Phantom validation and clinical data. Myocardial velocity and deformation imaging symposium, Leuven, 2009.

R. Faludi, M. Szulik, J. D'hooge, G. Pedrizzetti, F. van de Werf, J.-U. Voigt: Echo Particle Image Velocimetry: A new tool to assess intracavitary flow patterns. Annual Meeting of the German Cardiac Society, Mannheim, 2009.

R. Faludi, A. Walker, G. Pedrizzetti, J. Engvall, J.-U. Voigt: Can feature tracking correctly detect motion patterns as they occur in blood inside heart chambers? Validation of echocardiographic particle image velocimetry using moving phantoms. Annual Meeting of the German Cardiac Society, Mannheim, 2009. (Poster)

R. Faludi, M. Szulik, G. Pedrizzetti, P. Herijgers, J.-U. Voigt: How do prosthetic mitral valves influence left ventricular flow patterns and energetics? An echocardiographic particle image velocimetry study in healthy subjects and patients with mitral prosthesis. Annual Meeting of the German Cardiac Society, Mannheim, 2009.

R. Faludi: Flow tracking - Patterns inside the heart. EUROECHO Congress, Madrid, 2009.

10. Acknowledgments

I would like to express my gratitude to all those who gave me the possibility to complete this thesis.

I am deeply grateful to my supervisors Prof. Dr. Tamás Simor and Prof. Dr. Erzsébet Rőth, whose stimulating suggestions and encouragement helped me in all the time of research for and writing of this thesis.

I am indebted to my professors who supervised my work abroad, namely Prof. Dr. Jens-Uwe Voigt and Prof. Jan D'hooge from the Catholic University Leuven, for teaching me professional science.

I thank my former professors, Prof. Dr. Gyula Mózsik and Prof. Dr. Lajos Papp as well as my recent chief Dr. Sándor Szabados for the continuing support.

My former and recent colleagues from the I. Department of Internal Medicine and Heart Institute supported me in my research work. I want to thank them for all their help, support, interest and valuable hints. Especially I am obliged to Dr. András Komócsi and Dr. Levente Tóth.

Especially, I would like to give my special thanks to my parents whose patient love enabled me to complete this work.